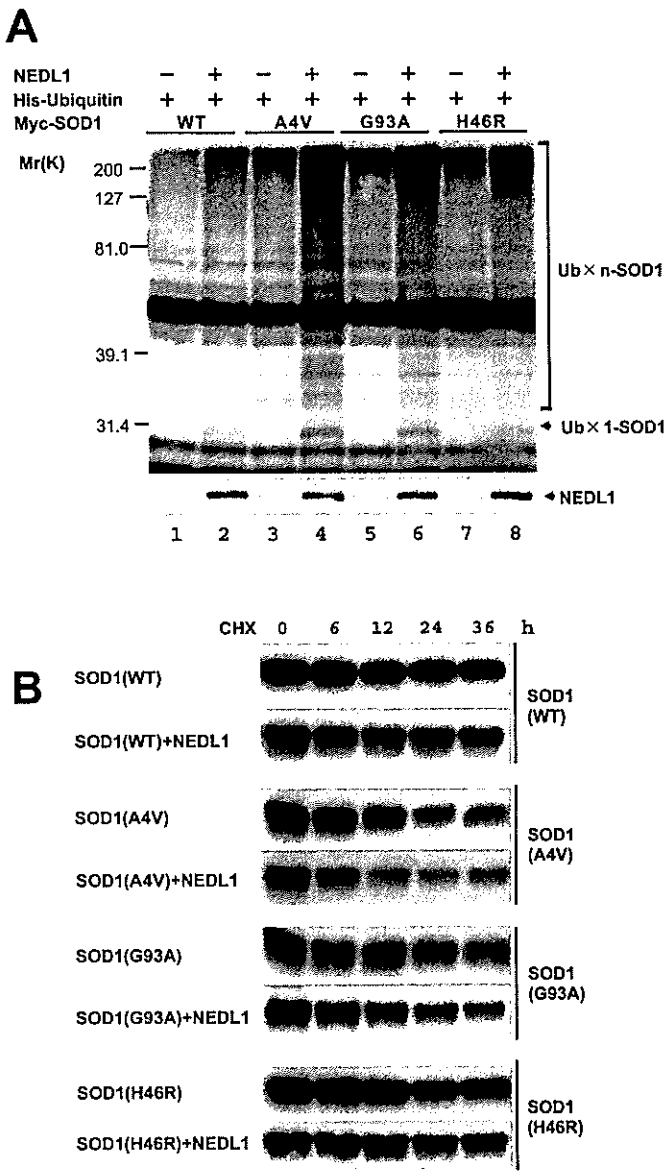

FIG. 4. **NEDL1-dependent ubiquitination and degradation of mutant forms of SOD1 correlate broadly with their respective clinical phenotypes.** *A*, NEDL1 ubiquitinates mutant SOD1 in a mutant type-dependent manner. COS-7 cells were transiently cotransfected with the indicated expression plasmids. Whole cell lysates from transfected COS-7 cells were immunoprecipitated with anti-Myc antibody, and immunoprecipitates were analyzed by Western blotting with anti-ubiquitin (*Ub*) antibody (*upper panel*). The *bracket* indicates slowly migrating ubiquitinated forms of SOD1. Whole cell lysates were analyzed by immunoblotting with anti-NEDL1 antibody to confirm the expression of transfected NEDL1 (*lower panel*). The running positions of molecular weight markers are indicated on the left. *B*, half-lives of wild-type (*WT*) and mutant SOD1 proteins in the presence or absence of NEDL1. Cell lysates were harvested from Neuro2a cells transfected with *SOD1* alone or with *SOD1* plus *NEDL1* at different time points as indicated after the addition of cycloheximide (*CHX*; final concentration of 50 μg/ml) and were analyzed for SOD1 protein levels by Western blotting with anti-FLAG antibody. In the presence of NEDL1, the half-lives of various mutant SOD1 proteins were reduced also roughly dependent on the disease severity of FALS (A4V > G93A > H46R).

wild-type). Thus, NEDL1 targeted mutant SOD1 for ubiquitin-mediated degradation in the cell in parallel with the binding intensity.

Immunohistochemistry—One of the characteristic cytopathological changes of mutant SOD1-linked FALS is the formation of neuronal Lewy body-like hyaline inclusions (LBHIs) that contain aggregates of SOD1 and ubiquitin (24). We therefore

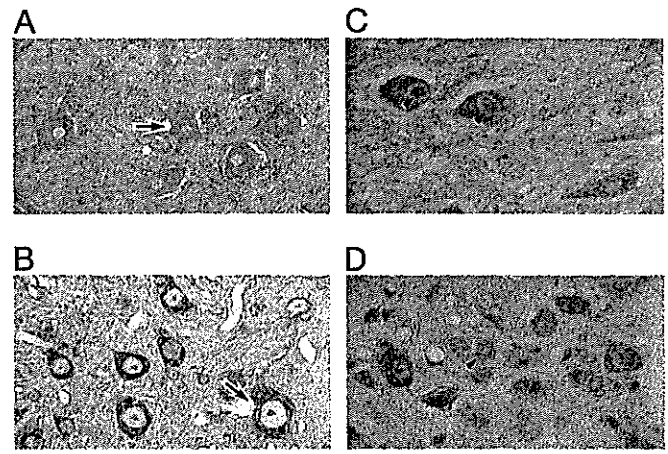

FIG. 5. **NEDL1 immunohistochemical analyses.** *A*, immunohistochemical analysis of NEDL1 in normal human spinal cord. NEDL1-positive anterior horn cells are evident (*arrow*), although the immunoreactivity for NEDL1 is somewhat faint. There was no counterstaining. Magnification ×520. *B*, NEDL1 immunohistochemistry in normal mouse spinal cord. Normal anterior horn cells are positive for NEDL1 (*arrow*). The section was counterstained with hematoxylin. Magnification ×750. *C*, immunostaining for NEDL1 in spinal cord LBHIs from an FALS patient with a frameshift 126 mutation in the *SOD1* gene. The NEDL1-positive reaction products were mostly restricted to the cores of the core and halo-type LBHIs (*arrowheads*). In the LBHI-bearing neurons and residual neurons, the antibody to NEDL1 also stained the neuronal cell body. There was no counterstaining. Magnification ×540. *D*, NEDL1 immunostaining in a spinal cord LBHI from an *SOD1*(H46R) transgenic mouse. An ill defined LBHI in the *SOD1*(H46R) transgenic mouse was positive for NEDL1; this ill defined LBHI shows a diffuse staining pattern (*arrowhead*). The staining intensity in the residual neurons stained by anti-NEDL1 antibody varied from neuron to neuron. The section was counterstained with hematoxylin. Magnification ×770.

performed immunostaining to determine whether the NEDL1 protein is included within the LBHIs of the spinal cord motor neurons obtained from two siblings with FALS caused by frameshift 126 mutation of SOD1 (11, 12). One case had neuropathological findings compatible with FALS with posterior column involvement, whereas the other had multisystem degeneration in addition to motor neuron disturbance. We also performed NEDL1 immunostaining in specimens obtained from mutant *SOD1*(H46R) transgenic mice at 180 days, by which time they show clinical motor signs in the hind limbs (13). The specificity of the NEDL1 staining was confirmed by pretreating the specimens with an excess of NEDL1 antigen. NEDL1 immunoreactivity in the spinal cords of the human control cases was identical to that of normal mice: immunoreactivity was identified predominantly in the cytoplasm of the neurons of the spinal cords (Fig. 5, *A* and *B*). The LBHIs in the anterior horn cells of two FALS patients and transgenic mice showed equivalent immunoreactivity for NEDL1. Although the intensity of NEDL1 immunoreactivity in neuronal LBHIs varied, most of the LBHIs were immunoreactive for NEDL1 (Fig. 5, *C* and *D*). The reaction products were generally restricted to the cores of the core and halo-type LBHIs that showed eosinophilic cores with pale peripheral halos upon hematoxylin and eosin staining (Fig. 5*C*); by contrast, immunopositive NEDL1 in ill defined LBHIs was distributed throughout the inclusions (Fig. 5*D*). NEDL1 immunoreactivity in the residual neurons in humans and mice was identified primarily in cell bodies. Thus, NEDL1 immunostaining was clearly positive in the FALS-related LBHIs that were also positive for ubiquitin and SOD1 (data not shown).

NEDL1 Targets Dishevelled-1 for Ubiquitin-mediated Protein Degradation—We next hypothesized that the physiological function of NEDL1 to mediate ubiquitination is interfered with

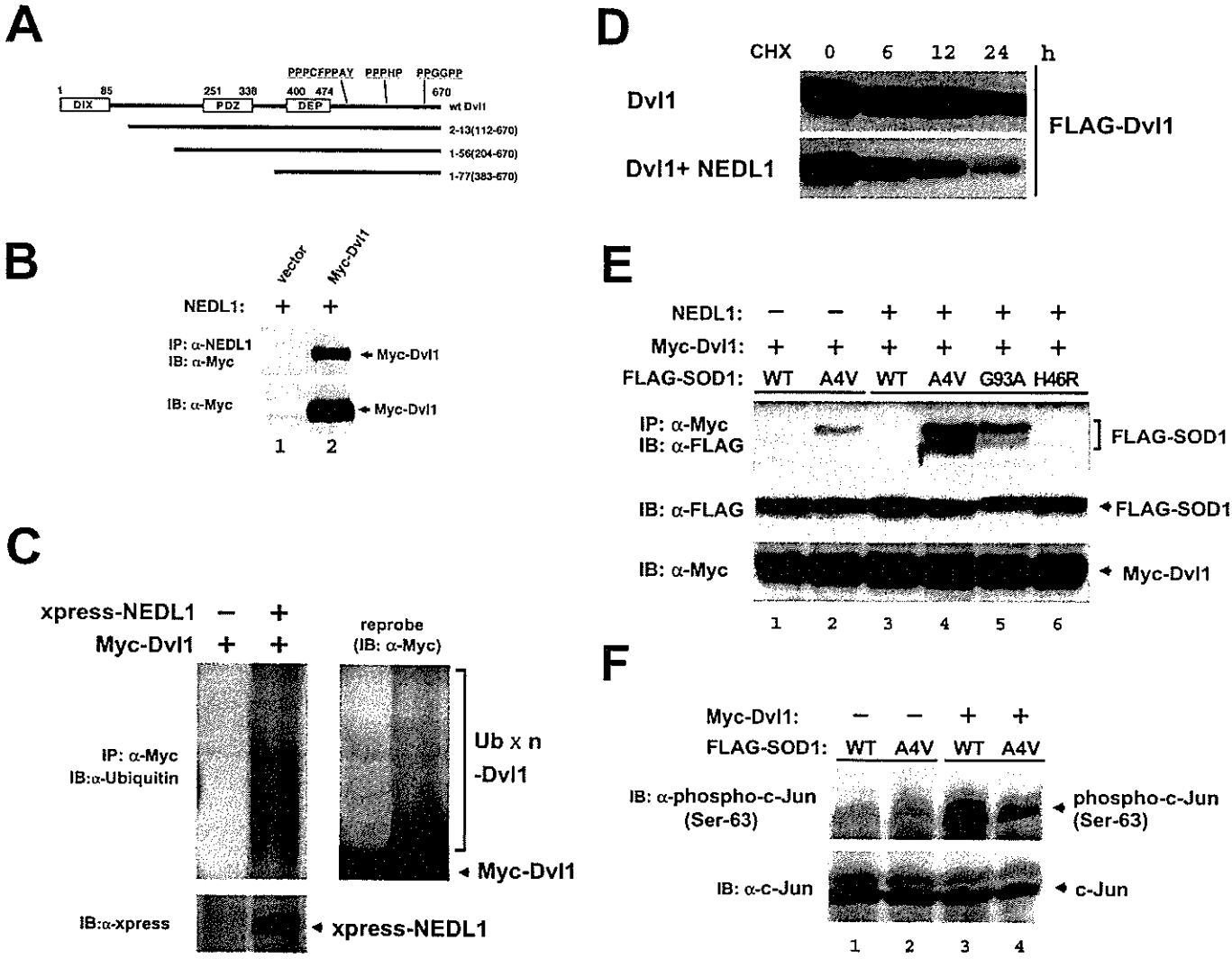

FIG. 6. **Dvl1 is a substrate of NEDL1, and its functions are disturbed by mutant SOD1(A4V).** *A*, schematic illustration of full-length Dvl1 and three clones obtained by yeast two-hybrid screening. Human Dvl1 consists of 670 amino acids and contains three conserved domains, including the DIX, PDZ, and DEP domains. Between the DEP domain and the C-terminal end, there are three proline-rich clusters, which might act as WW domain recognition sites. All three clones (clones 2–13, 1–56, 1–77) contain the DEP domain and these clusters. *B*, NEDL1 interacts with Dvl1. Myc-tagged Dvl1 was overexpressed together with NEDL1 in Neuro2a cells. Whole cell lysates were immunoprecipitated (*IP*) with anti-NEDL1 antibody, followed by immunoblotting (*IB*) with anti-Myc antibody (*upper panel*). The expression levels of Myc-tagged Dvl1 were analyzed by immunoblotting using anti-Myc antibody (*lower panel*). *C*, NEDL1 ubiquitinates Dvl1 in Neuro2a cells. The cells were transiently transfected with the indicated expression plasmids along with the ubiquitin expression plasmid in the presence or absence of the expression plasmid for XPRESS-tagged NEDL1. Whole cell lysates were immunoprecipitated with anti-Myc antibody and then immunoblotted with anti-ubiquitin antibody (*left panel*). The ladder of bands denoted by the *bracket* appeared to be ubiquitinated Dvl1. The expression of XPRESS-NEDL1 was analyzed by immunoblotting using anti-XPRESS antibody. The membrane was reprobed with anti-Myc antibody (*right panel*). *D*, Dvl1 is degraded by NEDL1. Neuro2a cells were transfected with the expression plasmid for FLAG-tagged Dvl1 with or without the NEDL1 expression plasmid. Transfected cells were harvested at different time points as indicated after the addition of cycloheximide (*CHX*; final concentration of 50 μg/ml), and Dvl1 protein levels were analyzed by Western blotting with anti-FLAG antibody. In the presence of NEDL1, the half-lives of FLAG-Dvl1 were significantly reduced. *E*, Dvl1 binds to mutant SOD1(A4V), and the degree of its binding is enhanced in the presence of NEDL1. Whole cell lysates prepared from COS-7 cells transfected with the indicated combinations of expression plasmids were subjected to immunoprecipitation and Western analyses as indicated. *F*, c-Jun phosphorylation by overexpression of Dvl1 is suppressed upon coexpression of mutant SOD1(A4V). Whole cell lysates from COS-7 cells transfected with the indicated combinations of expression plasmids were subjected to Western blotting with antibody against the phosphorylated form of c-Jun (*upper panel*) or with anti-c-Jun antibody (*lower panel*). *wt/WT*, wild-type.

by mutant SOD1. To test this hypothesis, we again performed yeast two-hybrid screening to obtain NEDL1-interacting molecules using the large region of NEDL1 (amino acids 382–1448) as bait. Of 396 His and β-galactosidase double-positive clones, 282 clones were subjected to DNA sequencing, and we identified Dvl1 (three clones). Human Dvl1 is a 670-amino acid protein with three conserved domains: a DIX domain, which is required for canonical Wnt/T-cell factor signaling; a PDZ domain, which is a target of both Stbm and casein kinase I binding; and a DEP domain, which is responsible for Dvl membrane localization during planar cell polarity signaling (25–27). Between the DEP domain and C-terminal end, there are three proline-rich clusters unique to mammalian Dvl1, which presumably act as the WW domain recognition sites. All three clones (clones 2–13, 1–56, and 1–77) contain the DEP domain and proline-rich clusters, suggesting that NEDL1 interacted with Dvl1 in the C-terminal half (Fig. 6*A*). In Neuro2a cells, NEDL1 co-immunoprecipitated with Dvl1 (Fig. 6*B*) and ubiquitinated it for degradation (Fig. 6, *C* and *D*). Thus, Dvl1 may be one of the physiological targets of NEDL1 E3. As recent studies strongly suggest that the cytotoxicity of SOD1 mutants is responsible for their aggregate properties, incorporating other proteins essential for cells into their aggregates (28), we examined the association between mutant SOD1 and Dvl1,

both of which interact with NEDL1. Of interest, Dvl1 bound to mutant SOD1(A4V), and complex formation was increased in the presence of NEDL1 roughly proportionately to the disease severity of FALS caused by the particular SOD1 mutant (Fig. 6*E*). Dvl1 is known to transduce not only the Wnt/β-catenin/T-cell factor pathway, but also the JNK/c-Jun pathway (27). Therefore, we next examined whether the Dvl1-induced phosphorylation of c-Jun at Ser^{63} was affected by the tight complex formation induced by inclusion of mutant SOD1. As shown in Fig. 6*F*, c-Jun phosphorylation induced by overexpression of Dvl1 was significantly suppressed by coexpression with mutant SOD1(A4V) in COS-7 cells.

DISCUSSION

Our present results demonstrate that a novel HECT-type NEDL1 E3, which is preferentially expressed in neuronal tissues, specifically targets mutant forms of SOD1 for ubiquitination-mediated protein degradation. NEDL1 is also associated with TRAP-δ localized at the ER translocon. The TRAP complex has recently been shown to facilitate the initiation of protein translocation in a substrate-specific manner (29). The NEDL1·TRAP-δ complex recognizes mutant (but not wild-type) SOD1, with a binding intensity that broadly parallels the disease severity of FALS. NEDL1 immunoreactivity was detected in the FALS-related LBHIs in the spinal cord ventral horn motor neurons, suggesting that, although mutant SOD1 is ubiquitinated for degradation by NEDL1, the mutant SOD1·NEDL1·TRAP-δ complex aggregates within the LBHIs. It is also conceivable that fragmentation of the Golgi apparatus reported in ALS patients and transgenic mice might be related to this aggregation (30, 31). These findings suggest possible hypotheses for the role of NEDL1 in the pathogenesis of FALS: 1) NEDL1, alone or with TRAP-δ, ubiquitinates and aggregates mutant SOD1, thereby decreasing the function of mutant SOD1; 2) NEDL1 and TRAP-δ form aggregates with mutant SOD1 that induce fragmentation of the Golgi apparatus, leading to neuronal apoptosis; 3) formation of these aggregates causes dysfunction of NEDL1 and/or TRAP-δ, and this, in turn, induces disturbances that ultimately cause motor neuron death; and 4) the mutant SOD1·NEDL1·TRAP-δ aggregates trap and inactivate unknown factor(s) such as molecular chaperones whose normal function is important for motor neuron viability.

To further understand the role of NEDL1 in motor neuron death, we searched for the physiological targets of NEDL1 and identified Dvl1. As expected, Dvl1 is ubiquitinated for degradation by NEDL1. Surprisingly, however, Dvl1 also interacts with mutant SOD1 in the presence of NEDL1 roughly proportionately to the disease severity of FALS caused by the particular SOD1 mutant. Dvl1, an essential multimodule signal transducer localized in the cellular cytosol and cytoskeleton, mediates planar cell polarity signaling as well as canonical Wnt/β-catenin signaling (27, 32). In mammals, three Dvl family members have so far been reported, and the level of Dvl1 expression is high in neuronal tissues (33). As far as we know, NEDL1 is the first E3 for Dvl1, interacting with the C-terminal region containing three proline-rich clusters. A recent report suggests that Dvl1 regulates microtubule stability through inhibition of glycogen synthase kinase-3β (34). Because cytoskeletal abnormalities have been reported in ALS motor neurons (35), it is possible that the effect of mutant SOD1 on NEDL1-mediated Dvl1 degradation is involved in the motor neuron death. Furthermore, Dvl1 is abundant in the postsynaptic membrane region at the neuromuscular junction (36) that is reported to be involved in several neurodegenerative disorders (37, 38). Of interest, *Dvl1* is mapped to chromosome 1p36, which is a commonly deleted region in many human cancers, including neuroblastoma (39). As NEDL1 is highly expressed in neuroblastomas with favorable prognosis, which have a tendency to differentiate and/or regress, NEDL1 may be involved in the regulation of neuronal differentiation and survival possibly by controlling Dvl1.

NEDL1, TRAP-δ, mutant SOD1, and Dvl1 appear to form a complex roughly proportionately to the disease severity of FALS caused by the particular SOD1 mutant. Our present observations strongly suggest that NEDL1 may be a quality control E3 recognizing misfolded mutant SOD1 (40). The association between mutant SOD1 and NEDL1 may induce the conformational change in the NEDL1 protein to increase the binding intensity with other physiological targets such as TRAP-δ (not ubiquitinated) and Dvl1 (ubiquitinated). This may lead to tight complex formation especially when the proteasome activity is impaired. It has been reported that the expression and function of proteasomes decrease with age in the spinal cord (7). Okado-Matsumoto and Fridovich (41) have also found that complex formation between mutant SOD1 and heat shock proteins leads to protein aggregates. Because our data show that the ER translocon component TRAP-δ is involved, aggregate formation may occur at the sites of the ER or Golgi apparatus or even at other cellular sites. The complex formation including NEDL1 and mutant SOD1 may conversely affect the physiological function of NEDL1, as demonstrated by a decrease in Dvl1-induced phosphorylation of c-Jun.

Recently, the RING finger-type E3 Dorfin has been reported to ubiquitinate mutant SOD1 for degradation (42). However, NEDL1 and Dorfin appear to be different in several aspects. First, NEDL1 is expressed specifically in neuronal tissues, including the spinal cord, whereas Dorfin is ubiquitously expressed in most human tissues. Second, both interaction between NEDL1 and mutant SOD1 and ubiquitination of the latter by NEDL1 roughly parallel the disease severity caused by the particular SOD1 mutant, whereas Dorfin similarly ubiquitinates mutant forms of SOD1. In addition, we have identified Dvl1 and TRAP-δ as cellular target proteins of NEDL1, whereas the physiological targets of Dorfin have never been reported. It is probable that there are some other E3 ligases targeting mutant SOD1. However, the molecular characteristics, including tissue-specific expression, subcellular localization, and age-dependent expression, might be important in the development of the FALS phenotype.

In conclusion, we have identified a novel neuronal E3 (NEDL1) that interacts with TRAP-δ and also binds to and ubiquitinates Dvl1 for degradation. Strikingly, NEDL1 targets and ubiquitinates mutant (but not wild-type) SOD1 for degradation. NEDL1 may normally function in the quality control of cellular proteins by eliminating misfolded proteins such as mutant SOD1, possibly via a mechanism analogous to that of ER-associated degradation (43–45). NEDL1 appears to complex tightly with mutant SOD1, Dvl1, and TRAP-δ, forming aggregates with species of mutant SOD1 that have escaped ubiquitin-mediated degradation. The NEDL1 function that affects the activities of the target proteins may also be modulated by mutant SOD1. All of these might contribute to the pathogenesis of FALS; further elucidation of the molecular mechanism of formation of this complex and its pathogenicity may provide insights into motor neuron death in ALS as well as possible new therapeutic strategies for ALS.

Acknowledgments—We thank Robert H. Brown, Jr. (Harvard Medical School) for critical comments and reading the manuscript. We also thank M. Ohira and Y. Nakamura for helping with cDNA cloning and sequencing; K. Watanabe and M. Suzuki for making plasmid constructs; M. Nagai and M. Kato for helping with immunohistochemical studies; S. Hatakeyama, M. Matsumoto, and K. Nakayama

for ubiquitination assay instruction; and S. Sakiyama for reading the manuscript.

REFERENCES

1. Rosen, D. R., Siddique, T., Patterson, D., Figlewicz, D. A., Sapp, P., Hentati, A., Donaldson, D., Goto, J., O'Regan, J. P., Deng, H. X., Rahmani, Z., Krizus, A., McKenna-Yasek, D., Cayabyab, A., Gaston, S. M., Berger, R., Tanzi, R. E., Halperin, J. J., Herzfeldt, B., van den Bergh, R., Hung, W.-Y., Bird, T., Deng, G., Mulder, D. W., Smyth, C., Laing, N. G., Soriano, E., Pericak-Vance, M. A., Haines, J., Rouleau, G. A., Gusella, J. S., Horvitz, H. R., and Brown, R. H., Jr. (1993) *Nature* **364,** 59–62
2. Deng, H. X., Hentati, A., Tainer, J. A., Iqbal, Z., Cayabyab, A., Hung, W.-Y., Getzoff, E. D., Hu, P., Herzfeldt, B., Roos, R. P., Warner, C., Deng, G., Soriano, E., Smyth, C., Parge, H. E., Ahmed, A., Roses, A. D., Hallewell, R., Rericak-Vance, M. A., and Siddique, T. (1993) *Science* **261,** 1047–1051
3. Cleveland, D. W., and Liu, J. (2001) *Nat. Med.* **6,** 1320–1321
4. Brown, R. H., Jr., and Robberecht, W. (2001) *Semin. Neurol.* **21,** 131–139
5. Cluskey, S., and Ramsden, D. B. (2001) *Mol. Pathol.* **54,** 386–392
6. Orrell, R. W., and Figlewicz, D. A. (2001) *Neurology* **57,** 9–17
7. Keller, J. N., Huang, F. F., and Markesbery, W. R. (2000) *Neuroscience* **98,** 149–156
8. Hoffman, E. K., Wilcox, H. M., Scott, R. W., and Siman, R. (1996) *J. Neurol. Sci.* **139,** 15–20
9. Kunst, C. B., Mezey, E., Brownstein, M. J., and Patterson, D. (1997) *Nat. Genet.* **15,** 91–94
10. Hartmann, E., Gorlich, D., Kostka, S., Otto, A., Kraft, R., Knespel, S., Burger, E., Rapoport, T. A., and Prehn, S. (1993) *Eur. J. Biochem.* **214,** 375–381
11. Kato, S., Shimoda, M., Watanabe, Y., Nakashima, K., Takahashi, K., and Ohama, E. (1996) *J. Neuropathol. Exp. Neurol.* **55,** 1089–1101
12. Kato, S., Hayashi, H., Nakashima, K., Nanba, E., Kato, M., Hirano, A., Nakano, I., Asayama, K., and Ohama, E. (1997) *Am. J. Pathol.* **151,** 611–620
13. Nagai, M., Aoki, M., Miyoshi, I., Kato, M., Pasinelli, P., Kasai, N., Brown, R. H., Jr., and Itoyama, Y. (2001) *J. Neurosci.* **21,** 9246–9254
14. Nakagawara, A. (1998) *Med. Pediatr. Oncol.* **31,** 113–115
15. Harvey, K. F., and Kumar, S. (1999) *Trends Cell Biol.* **9,** 166–169
16. Kumar, S., Tomooka, Y., and Noda, M. (1992) *Biochem. Biophys. Res. Commun.* **30,** 1155–1161
17. Kato, S., Takikawa, M., Nakashima, K., Hirano, A., Cleveland, D. W., Kusaka, H., Shibata, N., Kato, M., Nakano, I., and Ohama, E. (2000) *Amyotroph. Lateral Scler. Other Motor Neuron Disord.* **1,** 163–184
18. Orrell, R. W. (2000) *Neuromuscul. Disord.* **10,** 63–68
19. Cudkowicz, M. E., McKenna-Yasek, D., Sapp, P. E., Chin, W., Geller, B., Hayden, D. L., Schoenfeld, D. A., Hosler, B. A., Horvitz, H. R., and Brown, R. H., Jr. (1997) *Ann. Neurol.* **41,** 210–221
20. Ratovitski, T., Corson, L. B., Strain, J., Wong, P., Cleveland, D. W., Culotta, V. C., and Borchelt, D. R. (1999) *Hum. Mol. Genet.* **8,** 1451–1460
21. Aoki, M., Ogasawara, M., Matsubara, Y., Narisawa, K., Nakamura, S., Itoyama, Y., and Abe, K. (1993) *Nat. Genet.* **5,** 323–324
22. Kato, M., Aoki, M., Ohta, M., Nagai, M., Ishizaki, F., Nakamura, S., and Itoyama, Y. (2001) *Neurosci. Lett.* **312,** 165–168
23. Andersen, P. M., Forsgren, L., Binzer, M., Nilsson, P., Ala-Hurula, V., Keranen, M. L., Bergmark, L., Saarinen, A., Haltia, T., Tarvainen, I., Kinnunen, E., Udd, B., and Marklund, S. L. (1996) *Brain* **119,** 1153–1172
24. Shibata, N., Hirano, A., Kobayashi, M., Siddique, T., Deng, H. X., Hung, W.-Y., Kato, T., and Asayama, K. (1996) *J. Neuropathol. Exp. Neurol.* **55,** 481–490
25. Sussman, D. J., Klingensmith, J., Salinas, P., Adams, P. S., Nusse, R., and Perrimon, N. (1994) *Dev. Biol.* **166,** 73–86
26. Wodarz, A., and Nusse, R. (1998) *Annu. Rev. Cell Dev. Biol.* **14,** 59–88
27. Boutros, M., Paricio, N., Strutt, D. I., and Mlodzik, M. (1998) *Cell* **94,** 109–118
28. Julien, J. P. (2001) *Cell* **104,** 581–591
29. Fons, R. D., Bogert, B. A., and Hegde, R. S. (2003) *J. Cell Biol.* **160,** 529–539
30. Fujita, Y., Okamoto, K., Sakurai, A., Gonatas, N. K., and Hirano, A. (2000) *J. Neurol. Sci.* **174,** 137–140
31. Mourelatos, Z., Gonatas, N. K., Stieber, A., Gurney, M. E., and Dal Canto, M. C. (1996) *Proc. Natl. Acad. Sci. U. S. A.* **93,** 5472–5477
32. Wharton, K. A., Jr. (2003) *Dev. Biol.* **253,** 1–17
33. Tsang, M., Lijam, N., Yang, Y., Beier, D. R., Wynshaw-Boris, A., and Sussman, D. J. (1996) *Dev. Dyn.* **207,** 253–262
34. Krylova, O., Messenger, M. J., and Salinas, P. C. (2000) *J. Cell Biol.* **151,** 83–94
35. Julien, J. P., and Beaulieu, J. M. (2000) *J. Neurol. Sci.* **180,** 7–14
36. Luo, Z. G., Wang, Q., Zhou, J. Z., Wang, J., Luo, Z., Liu, M., He, X., Wynshaw-Boris, A., Xiong, W. C., Lu, B., and Mei, L. (2002) *Neuron* **35,** 489–505
37. De Ferrari, G. V., and Inestrosa, N. C. (2000) *Brain Res. Brain Res. Rev.* **33,** 1–12
38. Kaytor, M. D., and Orr, H. T. (2000) *Curr. Opin. Neurobiol.* **12,** 275–278
39. Versteeg, R., Caron, H., Cheng, N. C., van der Drift, P., Slater, R., Westerveld, A., Voute, P. A., Delattre, O., Laureys, G., van Roy, N., and Speleman, F. (1995) *Eur. J. Cancer* **31,** 538–541
40. Murata, S., Minami, Y., Minami, M., Chiba, T., and Tanaka, K. (2001) *EMBO Rep.* **2,** 1133–1138
41. Okado-Matsumoto, A., and Fridovich, I. (2002) *Proc. Natl. Acad. Sci. U. S. A.* **99,** 9010–9014
42. Niwa, J., Ishigaki, S., Hishikawa, N., Yamamoto, M., Doyu, M., Murata, S., Tanaka, K., Taniguchi, N., and Sobue, G. (2002) *J. Biol. Chem.* **277,** 36793–36798
43. Mori, K. (2000) *Cell* **101,** 451–454
44. Travers, K. J., Patil, C. K., Wodicka, L., Lockhart, D. J., Weissman, J. S., and Walter, P. (2000) *Cell* **101,** 249–258
45. Wickner, S., Maurizi, M. R., and Gottesman, S. (1999) *Science* **286,** 1888–1893
46. Borchelt, D. R., Lee, M. K., Slunt, H. S., Guarnieri, M., Xu, Z. S., Wong, P. C., Brown, R. H., Jr., Price, D. L., Sisodia, S. S., and Cleveland, D. W. (1994) *Proc. Natl. Acad. Sci. U. S. A.* **16,** 8292–8296

THE JOURNAL OF BIOLOGICAL CHEMISTRY

Vol. 279, No. 24, Issue of June 11, pp. 25549–25561, 2004
Printed in U.S.A.

Polo-like Kinase 1 (Plk1) Inhibits p53 Function by Physical Interaction and Phosphorylation*

Received for publication, December 26, 2003, and in revised form, March 11, 2004
Published, JBC Papers in Press, March 15, 2004, DOI 10.1074/jbc.M314182200

Kiyohiro Ando‡§¶, Toshinori Ozaki‡¶, Hideki Yamamoto‡, Kazushige Furuya‡, Mitsuchika Hosoda‡, Syunji Hayashi‡, Masahiro Fukuzawa§, and Akira Nakagawara‡‖

From the ‡Division of Biochemistry, Chiba Cancer Center Research Institute, Chiba 260-8717, Japan and the §First Department of Surgery, Nihon University School of Medicine, Tokyo 173-8610, Japan

Polo-like kinase 1 (Plk1) has an important role in the regulation of M phase of the cell cycle. In addition to its cell cycle-regulatory function, Plk1 has a potential role in tumorigenesis. Here we found for the first time that Plk1 physically binds to the tumor suppressor p53 in mammalian cultured cells, and inhibits its transactivation activity as well as its pro-apoptotic function. During the cisplatin-induced apoptosis in human neuroblastoma SH-SY5Y cells, the expression level of Plk1 was significantly decreased both at mRNA and protein levels, whereas cisplatin treatment caused a remarkable stabilization of p53. Systematic immunoprecipitation analyses using a series of deletion mutants of p53 revealed that a sequence-specific DNA-binding region of p53 is required and sufficient for the physical interaction with Plk1. The ectopically overexpressed Plk1 was co-localized with the endogenous p53 in mammalian cell nucleus, as shown by confocal laser microscopy. Expression of exogenous Plk1 and p53 in p53-deficient lung carcinoma H1299 cells greatly decreased the p53-mediated transcription from the p53-responsive *p21*^{WAF1}, *MDM2*, and *BAX* promoters, whereas the kinase-deficient mutant form of Plk1 failed to reduce the transcriptional activity of p53. Consistent with the luciferase reporter analysis, Plk1 had an ability to block the p53-dependent induction of the endogenous p21^{WAF1}. In addition, Plk1 inhibited the pro-apoptotic function of p53 in H1299 cells. Intriguingly, Plk1-mediated repression of p53 was attenuated with ATM. Thus, our present findings strongly suggest that p53 is a critical target of Plk1, and its function is abrogated through the physical interaction with Plk1.

The polo-like kinases (Plks)[1] are structurally and functionally related to the *Drosophila* polo serine/threonine (Ser/Thr) kinase (1), and are evolutionarily well conserved from yeast to mammals. A high degree of amino acid sequence similarity is detected within a catalytic domain and a unique noncatalytic domain (termed the polo-box) located at the NH_2- and COOH-terminal region, respectively (2). It has been shown that the polo-box is critical for the correct subcellular localization of Plks (3, 4), and the COOH-terminal region containing the polo-box serves to regulate its kinase activity (5). A growing body of evidence obtained in various experimental systems suggests that Plks play an important role in the regulation of a variety of M-phase-specific events including entry into and exit from mitosis (1, 6–8). In addition to their critical role during the G_2/M transition, Plks might be also required for G_1/S phase transition (9, 10).

In mammalian cells, there exist at least three Plk family members including Plk1, Plk2, and Plk3. Plk1 (also referred to as Plk) has been identified as a serine/threonine kinase that displays an extensive amino acid sequence homology to *Drosophila* polo (2, 9, 11–13), whereas Plk2 (alternatively named Snk) and Plk3 (alternatively termed as proliferation related kinase, Prk) have been originally shown to be transcriptionally induced in response to mitogens (14, 15). In mammalian cultured cells, the amounts of Plk1 mRNA and protein are regulated in a cell cycle-dependent manner, rising from a very low level in G_1 phase to a maximal level during G_2/M phase (11, 12). The kinase activity of Plk1 is regulated by its phosphorylation and peaks at M phase (16–18). Recently, it has been shown that the kinase activity of Plk1 is inhibited in response to DNA damage in mammalian cultured cells and this inhibition occurs in an ATM-dependent manner (19, 20). Plk1 phosphorylates various substrate proteins including cyclin B1 and Cdc25C. At the onset of mitosis, Plk1 phosphorylated cyclin B1 and promoted rapid nuclear translocation of an active Cdc2-cyclin B1 complex (21, 22). In addition, Toyoshima-Morimoto *et al.* (23) has found that, during G_2/M phase, Plk1 is capable of phosphorylating Cdc25C, which dephosphorylates and directly activates the Cdc2-cyclin B1 complex, and regulating the nuclear entry of Cdc25C. In contrast to Plk1, the expression level of Plk3 remains constant during the cell cycle progression and its kinase activity peaks during late S and G_2 phase (24, 25). Xie *et al.* (26) found that the kinase activity of Plk3 is rapidly increased in response to DNA damage in an ATM-dependent fashion.

In addition to the potential cell cycle-regulatory role, Plk1 has been implicated in the genesis and/or progression of tumors. *Plk1* was overexpressed in rapidly proliferating cells as well as various human primary tumors (27), suggesting that the expression level of *Plk1* is tightly linked to proliferation and could be used as a negative prognostic indicator for various

* This work was supported in part by a grant-in-aid from the Ministry of Health and Welfare for a New 10-Year Strategy for Cancer Control, a grant-in-aid for Scientific Research on Priority Areas, a grant-in-aid for Scientific Research (B) from the Ministry of Education, Science, Sports and Culture, Japan, and the Hisamitsu Pharmaceutical Company. The costs of publication of this article were defrayed in part by the payment of page charges. This article must therefore be hereby marked "*advertisement*" in accordance with 18 U.S.C. Section 1734 solely to indicate this fact.

¶ Both authors contributed equally to this work.

‖ To whom correspondence should be addressed: Division of Biochemistry, Chiba Cancer Center Research Institute, 666-2 Nitona, Chuoh-ku, Chiba 260-8717, Japan. Tel.: 81-43-264-5431; Fax: 81-43-265-4459; E-mail: akiranak@chiba-ccri.chuo.chiba.jp.

[1] The abbreviations used are: Plk, polo-like kinase; ATM, ataxia telangiectasia mutated; GFP, green fluorescence protein; GST, glutathione *S*-transferase; NLS, nuclear localization signal; NMS, normal mouse serum; PBS, phosphate-buffered saline; TBS, Tris-buffered saline; TK, thymidine kinase; RT, reverse transcriptase.

tumors (28–30). Consistent with these observations, constitutive overexpression of Plk1 in NIH3T3 cells resulted in the oncogenic focus formation and induction of tumor growth in nude mice (10). Down-regulation of the endogenous *Plk1* by using several antisense oligonucleotides targeted to *Plk1* induced growth inhibition in certain cancerous cells (31). Additionally, treatment of the cells with small interfering RNA targeted against *Plk1* caused the cell cycle arrest and apoptosis (32, 33). Of note, Liu and Erikson (33) reported that the tumor suppressor p53 might be involved in the Plk1 depletion-induced apoptosis. Recently, Plk1 has also been reported to have an ability to phosphorylate p53 *in vitro*, however, it is still unknown whether there exists a functional association between Plk1 and p53 (26). In sharp contrast to *Plk1*, the expression level of *Plk3* was significantly down-regulated in several human primary tumors including lung carcinomas and head and neck squamous cell carcinomas, as compared with their corresponding normal tissues (34, 35). Overexpression of Plk3 in mammalian cultured cells inhibited proliferation and induced apoptosis (36). Furthermore, it has been demonstrated that Plk3 physically interacts with p53 and phosphorylates the Ser^{20} of p53, which might result in the enhancement of its activity. These suggest that Plk1 and Plk3 play a differential role in regulating cell proliferation and oncogenesis, and that p53 participates in Plk3-dependent growth inhibition and/or apoptosis (25, 26, 36, 37).

In the present study, we examined the physical and functional interaction between Plk1 and p53. We found that Plk1 binds to the sequence-specific DNA-binding domain of p53, and inhibits the p53-dependent transcriptional activation as well as pro-apoptotic function. Intriguingly, overexpression of ATM abrogated the Plk1-mediated inhibitory effect on p53. These results suggest that the Plk1-mediated negative regulation of p53 might be a fundamental mechanism for the Plk1-induced oncogenesis.

EXPERIMENTAL PROCEDURES

Tumor Samples—Surgically resected tumor tissues including three lung adenocarcinomas, two gastric adenocarcinomas, one uterus carcinoma, two bladder carcinomas, and their corresponding normal tissues used in this study were obtained as frozen specimens from the Tissue Bank in Chiba Cancer Center Hospital (Chiba, Japan). Six hepatoblastomas and their matched normal tissues were provided by the Japanese Study Group for Pediatric Liver Tumor.

Cell Culture—African green monkey kidney COS7 cells were maintained in Dulbecco's modified Eagle's medium supplemented with 10% heat-inactivated fetal bovine serum (Invitrogen) and penicillin (100 IU/ml)/streptomycin (100 μg/ml). Human neuroblastoma SH-SY5Y cells and human lung carcinoma H1299 cells were grown in RPMI 1640 medium containing 10% heat-inactivated fetal bovine serum and antibiotic mixture. Cultures were maintained at 37 °C in a water-saturated atmosphere of 5% CO_2 in air.

Transfection—COS7 cells were transfected with the indicated expression plasmids using FuGENE 6 transfection reagent (Roche Applied Science) in a 6-cm diameter culture dish in accordance with the manufacturer's specifications. Transfection of H1299 cells was conducted by lipofection with LipofectAMINE transfection reagent (Invitrogen) in a 12-well plate according to the manufacturer's instructions.

RT-PCR—Total RNA was prepared from SH-SY5Y cells exposed to cisplatin by using the RNeasy Mini Kit (Qiagen Inc., Valencia, CA) according to the manufacturer's protocol, and subjected to synthesis of the first strand cDNA with random primers and a SuperScript II reverse transcriptase (Invitrogen) at 42 °C for 1 h. When the reaction was complete, the cDNA was amplified in a final volume of 15 μl of reaction mixture containing 100 μM of each deoxynucleoside triphosphate, 1× PCR buffer, 1 μM of each primer, and 0.2 units of rTaq DNA polymerase (Takara, Ohtsu, Japan). The primers for *p53* amplification were 5′-ATTTGATGCTGTCCCCGGACGATATTGAAC-3′ and 5′-ACCCTTTTTGGACTTCAGGTGGCTGGAGTG-3′. The primers for $p21^{WAF1}$ amplification were 5′-ATGAAATTCACCCCCTTTCC-3′ and 5′-CCCTAGGCTGTGCTCACTTC-3′. The primers for *Plk1* amplification were 5′-ATCACCTGCCTGACCATTCCACCAAGG-3′ and 5′-AATTGCGGAAATATTTAAGGAGGGTGATCT-3′. The primers for *Plk3* amplification were 5′-GCGCGAGAAGATCCTAAATG-3′ and 5′-GATCTGCCGCAGGTAGTAGC-3′. The primers for *GAPDH* amplification were 5′-ACCTGACCTGCCGTCTAGAA-3′ and 5′-TCCACCACCCTGTTGCTGTA-3′. The PCR-amplified products were separated by electrophoresis on a 1.5% agarose gel and visualized by ethidium bromide post-staining.

Generation of FLAG-tagged Expression Constructs—The FLAG-tagged human *Plk1* construct was generated by PCR amplification using the cDNA derived from primary hepatoblastoma as a template. The forward and reverse primers used in the PCR were 5′-CCGCTCGAGAGTGCTGCAGTGACTGCAGGGAAG-3′ and 5′-CTAGTCTAGATTAGGAGGCCTTGAGACGGTTGCT-3′. The underlined nucleotides represent the XhoI restriction sites in the forward primer and the XbaI restriction site in the reverse primer. The PCR product was subcloned into pGEM-T Easy (Promega Corp., Madison, WI), and its nucleotide sequence was verified by automated dideoxy terminator cycle sequencing. The PCR product was digested with XhoI and XbaI, and inserted between the XhoI to XbaI sites in the pcDNA3-FLAG expression plasmid in-frame to the downstream of the FLAG tag to give pcDNA3-FLAG-*Plk1*.

Construction of the Deletion Mutants of p53 and Plk1—The *p53* deletion mutants, *p53*-(1–359), *p53*-(1–292), and *p53*-(1–101) were generated by using the forward primer 5′-CCCAAGCTTGGGATGGAGGAGCCGCAGTCAGATCCTAGCGTC-3′ (1F) in combination with the reverse primers 5′-CCGGAATTCCGGTCATGGCTCCTTCCCAGCCTGGGCATCCTT-3′ (359R), 5′-CCGGAATTCCGGTCATTTCTTGCGGAGATTCTCTTCCTCTGT-3′ (292R) and 5′-CCGGAATTCCGGTCATTTCTGGGAAGGGACAGAAGATGACA-3′ (101R), respectively. *p53*-(102–393) was amplified by using the forward primer 5′-CCCAAGCTTGGGATGACCTACCAGGGCAGCTACGGTTTCCGTCT-3′ (102F) and the reverse primer 5′-CCGGAATTCCGGTCAGTCTGAGTCAGGCCCTTCTGTCTTGAACAT-3′ (393R). Each of the forward and reverse primers contained the HindIII and EcoRI restriction sites to facilitate the subsequent cloning step. Underlined nucleotides in the oligonucleotides listed above were HindIII or EcoRI sites. Amplified fragments were digested with HindIII and EcoRI, and subcloned directly into the identical restriction sites of pcDNA3 to give pcDNA3-*p53*-(1–359), pcDNA3-*p53*-(1–292), pcDNA3-*p53*-(1–101), and pcDNA3-*p53*-(102–393). All of the constructs were confirmed by sequence analysis. For the construction of the deletion mutants of Plk1, pcDNA3-FLAG-*Plk1* was digested with BamHI, BamHI and BstXI, or BamHI and NcoI. A restriction fragment encoding amino acid residues 1–401, 1–329, or 1–98 was purified from agarose gels, filled in the overhangs with Klenow, and then inserted in-frame into the enzymatically modified BamHI and XhoI sites of the pcDNA3-FLAG expression plasmid to give pcDNA3-FLAG-*Plk1*-(1–401), pcDNA3-FLAG-*Plk1*-(1–329), or pcDNA3-FLAG-*Plk1*-(1–98), respectively. DNA sequencing confirmed the authenticity of the expression plasmids prior to transfection.

Construction of the Kinase-deficient Mutant Form of Plk1—The K82M mutation was introduced into wild-type Plk1 by the PCR-based strategy using *PfuUltra*™ High Fidelity DNA polymerase (Stratagene, La Jolla, CA) according to the manufacturer's instructions. The following oligonucleotides were used: 5′-ATGATTGTGCCTAAGTCTCTGCTGCTCAAGCCGCA-3′ (underlined segment encodes Met at amino acid position 82) and 5′-GCCCGCGAACACCTCCTTGGTGTCCGCGTCCGAGA-3′. Nucleic acid sequencing was performed to verify the presence of the desired mutation and absence of random mutations. The amplified fragment that contains the K82M mutation was then digested with HindIII and NcoI, gel-purified, and ligated with the NcoI/XbaI restriction fragment containing the 3′-portion of the wild-type *Plk1* cDNA. The resulting entire cDNA encoding the full-length Plk1 carrying the amino acid substitution at position 82 was inserted in-frame into the HindIII and XbaI sites of the pcDNA3-FLAG expression plasmid to give pcDNA3-FLAG-*Plk1*(K82M).

Construction of the Expression Plasmid for Antisense Plk1—A full-length human *Plk1* cDNA was ligated into the pcDNA3 expression plasmid in a reverse orientation to give As-*Plk1*, and the product was evaluated by restriction digestion. To assess the effect of As-*Plk1* on the endogenous Plk1, whole cell lysates prepared from H1299 cells transfected with As-*Plk1* were analyzed for Plk1 by immunoblotting.

GST Pull-down Assay—Whole cell lysates prepared from COS7 cells expressing FLAG-Plk1 were incubated with 1 μg of GST or GST-p53 (Santa Cruz Biotechnologies, Santa Cruz, CA) immobilized on glutathione-Sepharose beads for 2 h at 4 °C. The beads were washed extensively with NETN buffer (50 mM Tris-Cl, pH 7.5, 150 mM NaCl, 0.1% Nonidet P-40, and 1 mM EDTA) containing 1 mM phenylmethylsulfonyl fluoride. The bound proteins were eluted with 2× SDS sample buffer by boiling

for 5 min, and separated by 10% SDS-polyacrylamide gel electrophoresis followed by immunoblotting.

Immunofluorescent Labeling and Confocal Microscopy—COS7 cells, cultured onto glass coverslips, were transiently transfected with the expression plasmid for FLAG-Plk1. Transfected cells were washed twice with 1× PBS and then fixed with 1× PBS containing 3.7% formaldehyde for 30 min at room temperature. After washing with 1× PBS, cells were permeabilized with 0.2% Triton X-100 for 5 min at room temperature and blocked for 1 h in 1× PBS containing 3% bovine serum albumin. Cells were then incubated with polyclonal anti-p53 antibody (Cell Signaling Technology, Inc., Beverly, MA) and monoclonal anti-FLAG antibody (M2, Sigma) for 1 h at room temperature. After incubation with primary antibodies, cells were washed twice with 1× PBS and incubated with fluorescein isothiocyanate- or rhodamine-conjugated secondary antibodies (Invitrogen) diluted 1:200 for 1 h at room temperature. Cell nuclei were stained with 4,6-diamidino-2-phenylindole at a final concentration of 1 μg/ml (Sigma). Cells were finally washed with 1× PBS, the coverslips were removed from the dishes, mounted onto slides, and observed under Fluoview laser scanning confocal microscope (Olympus, Tokyo, Japan).

Western Blot Analysis—Cells were transfected with the indicated combinations of the expression plasmids. Forty-eight hours after transfection, cells were extracted directly with the lysis buffer containing 25 mM Tris-HCl, pH 8.0, 137 mM NaCl, 2.7 mM KCl, 1% Triton X-100, 1 mM phenylmethylsulfonyl fluoride and protease inhibitor mixture (Sigma) and the whole cell lysates were sonicated for 10 s followed by centrifugation at 15,000 rpm for 10 min at 4 °C to remove insoluble materials. The protein concentrations were determined using the Bradford protein assay according to the instructions of the vendor (Bio-Rad). Equal amounts of the whole cell lysates (50 μg of protein) were boiled in an SDS sample buffer consisting of 62.5 mM Tris-HCl, pH 6.8, 2% SDS, 2% β-mercaptoethanol, and 0.01% bromphenol blue and subjected to 10% SDS-polyacrylamide gel electrophoresis under reducing conditions and then electrotransferred onto Immobilon-P membranes (Millipore, Bedford, MA) at room temperature for 1 h. The membranes were blocked with TBS-T (50 mM Tris-Cl, pH 7.6, 100 mM NaCl, and 0.1% Tween 20) containing 5% nonfat dry milk at room temperature for 1 h, and subsequently incubated for 1 h with monoclonal anti-Plk1 (PL2 and PL6, Zymed Laboratories, Inc., San Francisco, CA), monoclonal anti-p53 (DO-1, Oncogene Research Products, Cambridge, MA), monoclonal anti-FLAG antibody (M2, Sigma), monoclonal anti-Plk3 antibody (B37–2, BD Pharmingen), polyclonal antibody specific for p53 phosphorylated at Ser^{15} (Cell Signaling, Beverly, MA), polyclonal anti-$p21^{WAF1}$ antibody (H-164, Santa Cruz Biotechnologies), or polyclonal anti-actin antibody (20–33, Sigma) in TBS-T, followed by an incubation with horseradish peroxidase-conjugated goat anti-mouse or anti-rabbit secondary antibody (Jackson ImmunoResearch Laboratories, West Grove, PA) diluted at 1:2,000 for 1 h at room temperature. The membranes were washed extensively with TBS-T and protein bands were visualized by enhanced chemiluminescence (ECL) according to the manufacturer's instructions (Amersham Biosciences).

Subcellular Fractionation—Cells were fractionated into cytosolic and nuclear fractions as described previously (38). Briefly, cells were washed twice with ice-cold 1× PBS and lysed in lysis buffer containing 10 mM Tris-HCl, pH 7.5, 1 mM EDTA, 0.5% Nonidet P-40, and a protease inhibitor mixture (Sigma) for 30 min at 4 °C. Cell lysates were centrifuged at 15,000 × *g* for 10 min to collect the soluble fraction as cytosolic extracts. Insoluble materials were washed with the lysis buffer and further dissolved in 1× SDS sample buffer to collect the nuclear fraction. The nuclear and cytoplasmic fractions were subjected to immunoblot analysis using the anti-FLAG, monoclonal anti-lamin B (Ab-1, Oncogene Research Products), or monoclonal anti-Ras (RASK-3, Seikagaku Co., Tokyo, Japan) antibody.

Immunoprecipitation and Western Blot Analysis—For the immunoprecipitation of Plk1 and p53, COS7 cells were transiently transfected with 2 μg of the expression plasmid for FLAG-Plk1 using FuGENE 6 transfection reagent. Forty-eight hours post-transfection, cells were harvested and lysed by incubation with mixing in 400 μl of the EBC buffer (50 mM Tris-HCl, pH 7.5, 120 mM NaCl, 0.5% Nonidet P-40, and 1 mM phenylmethylsulfonyl fluoride) at 4 °C for 30 min. Whole cell lysates were then subjected to centrifugation at 15,000 × *g* for 20 min at 4 °C to remove insoluble materials. Equal amounts of whole cell lysates were precleared with 30 μl of a 50% slurry of protein A-Sepharose (Amersham Biosciences). After centrifugation, the supernatant was incubated with the normal mouse serum (NMS), monoclonal anti-FLAG, or monoclonal anti-p53 antibody at 4 °C for 2 h. The immunocomplexes were precipitated with the protein A-Sepharose beads at 4 °C for 30 min, which were then pelleted by centrifugation at 15,000 × *g* for 5 min. The precipitates were washed with the lysis buffer three times at 4 °C, resuspended in 30 μl of the SDS sample buffer, and treated at 100 °C for 5 min. Proteins were then resolved by 10% SDS-polyacrylamide gel electrophoresis, and transferred onto the Immobilon-P membranes. The protein complex was detected by Western blot analysis using the monoclonal anti-FLAG or monoclonal anti-p53 antibodies.

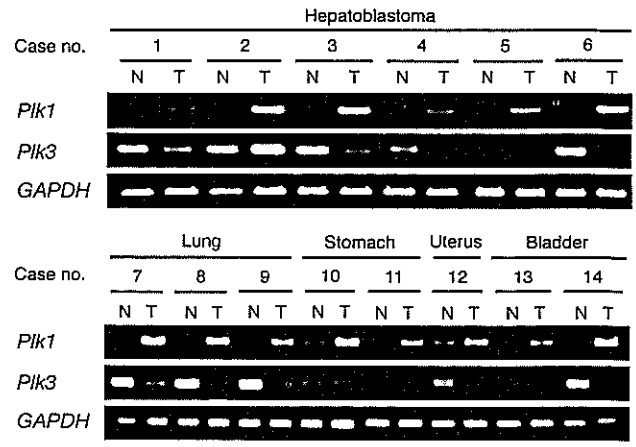

FIG. 1. **Expression of *Plk1* and *Plk3* mRNA in various human primary tumors and their corresponding normal tissues.** Total RNA (5 μg) prepared from the indicated tumor (*T*)-normal (*N*) paired samples was subjected to RT-PCR analysis for *Plk1* and *Plk3* mRNA expression using the specific primers as shown under "Experimental Procedures." The PCR-amplified products were analyzed by 1.5% agarose gel electrophoresis and visualized by ethidium bromide staining. Amplification of *GAPDH* was used as an internal control.

Luciferase Reporter Assays—p53-deficient H1299 cells were seeded in a 12-well tissue culture dish at a density of 5×10^4 cells/well. Cells were transfected with 100 ng of the p53-responsive luciferase reporter plasmid (*p21*, *MDM2*, or *BAX*), 10 ng of pRL-TK *Renilla* luciferase cDNA, and 25 ng of the expression plasmid for p53 together with or without increasing amounts of FLAG-Plk1 expression plasmid. The total amount of DNA was kept constant (510 ng) with pcDNA3 (Invitrogen) per transfection. Forty-eight hours post-transfection, transfected cells were washed twice with 1× PBS, and resuspended in passive lysis buffer (Promega Corp.). Both firefly and *Renilla* luciferase activities were assayed with the dual-luciferase reporter assay system (Promega Corp.) according to the manufacturer's instructions. The fluorescent light emission was determined by TD-20 luminometer (Turner Design, Sunnylvale, CA). The firefly luminescence signal was normalized based on the *Renilla* luminescence signal. The results were obtained from at least three sets of transfection and were presented as the mean ± S.D.

Cell Survival Assays—Cell viability was determined by a modified 3-(4,5-dimethylthiazol-2-yl)-2,5-diphenyltetrazolium bromide (MTT) assay. In brief, SH-SY5Y cells were seeded in 96-well microtiter plates (5×10^3 cell/well) with 100 μl of complete medium and allowed to attach. The next day, the medium were changed and cells were treated with cisplatin for 24 h. For the MTT assay, 10 μl of MTT solution was added to each well for 3 h at 37 °C. The absorbance readings for each well were carried out at 570 nm using the microplate reader (model 450, Bio-Rad).

Apoptotic Analysis—H1299 cells were transfected with a constant amount of the expression plasmid for green fluorescence protein (GFP) and p53 expression plasmid together with or without the expression plasmid encoding FLAG-Plk1. Forty-eight hours after transfection, transfected cells were identified by the presence of green fluorescence. To verify apoptosis, cell nucleus was stained with propidium iodide to reveal nuclear condensation and fragmentation. The number of GFP-positive cells with fragmented nuclei was scored, and presented as a percentage of the total number of fluorescent cells.

RESULTS

Expression of Plk1 and Plk3 in Paired Tumors and Adjacent Normal Tissues—It has been shown that the expression level of *Plk1* is increased in human tumors of various origins as compared with that of their corresponding normal tissues, suggesting that Plk1 contributes to the genesis and/or progression of tumors (13, 27–29). Recently, we have also identified *Plk1* as

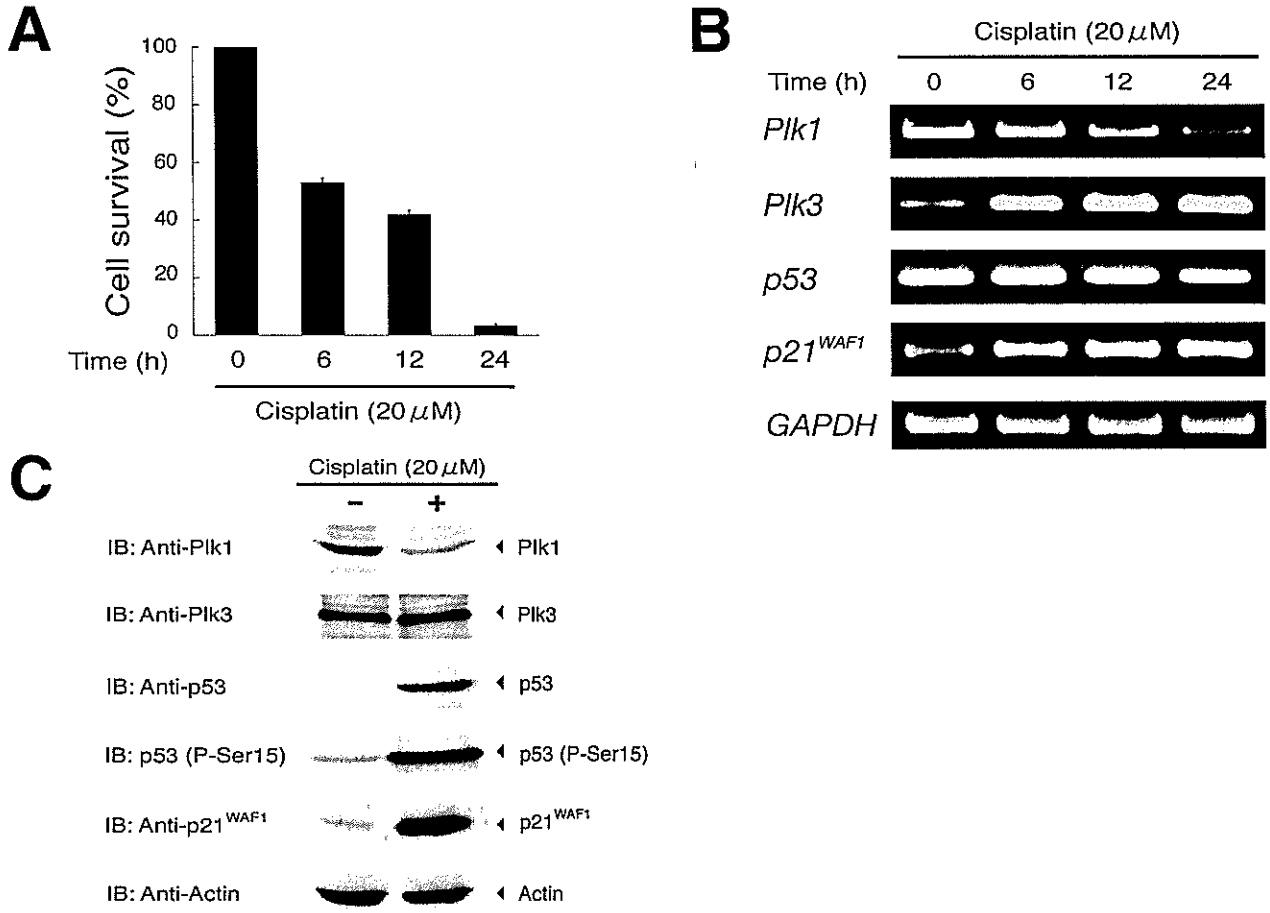

FIG. 2. **Down-regulation of *Plk1* during the cisplatin-induced apoptosis.** *A*, cell survival assays of SH-SY5Y cells treated with cisplatin. SH-SY5Y cells were exposed to cisplatin at a final concentration of 20 μM. At the indicated time periods after treatment with cisplatin, cell viability was determined by MTT assay. Data are presented as the mean ± S.D. of three independent experiments. *B*, RT-PCR analysis. Human neuroblastoma-derived SH-SY5Y cells were treated with or without cisplatin at a final concentration of 20 μM. At the indicated time periods after treatment with cisplatin, total RNA was prepared and subjected to RT-PCR analysis for the expression of *Plk1* (*1st panel*), *Plk3* (*2nd panel*), *p53* (*3rd panel*), and *p21*^{WAF1} (*4th panel*). Amplification of *GAPDH* serves as an internal control (*5th panel*). The PCR products were resolved in 1.5% agarose gels and visualized by ethidium bromide staining. *C*, Western blot analysis. Whole cell lysates were prepared from SH-SY5Y cells exposed to cisplatin for 24 h (at a final concentration of 20 μM) or left untreated and immunoblotted against anti-Plk1 (*1st panel*), anti-Plk3 (*2nd panel*), anti-p53 (*3rd panel*), antibody specific for p53 phosphorylated at Ser^{15} (*4th panel*), or with the anti-p21^{WAF1} antibody (*5th panel*). Immunoblotting for actin is shown as control for protein loading (*6th panel*).

one of the genes whose expression level is markedly elevated in human hepatoblastomas.[2] In contrast, *Plk3* expression is down-regulated in certain human tumors including lung carcinomas and head and neck squamous cell carcinomas (34, 35). To confirm the differential expression of both *Plk1* and *Plk3* in the same tissue samples, we examined their expression patterns among the indicated various paired cancer-normal tissues by RT-PCR. The levels of *GAPDH* mRNA were comparable between these paired samples. Consistent with the previous results, without exceptions, the expression levels of *Plk1* mRNA were significantly higher in cancerous tissues than those of their adjacent normal tissues (Fig. 1). On the other hand, *Plk3* was expressed at low levels in all the lung, uterus, and bladder carcinomas that we examined, as compared with their corresponding normal tissues, whereas a significant decrease in *Plk3* expression level in tumor tissues was undetectable in 2 of 6 hepatoblastomas and in 1 of 2 gastric carcinomas (Fig. 1). Thus, deregulated overexpression of *Plk1* is detected in all various types of tumors, whereas down-regulation of *Plk3* expression may be restricted to certain tumors.

[2] Yamada, S., Ohira, M., Horie, H., Ando, K., Takayasu, H., Suzuki, Y., Sugano, S., Hirata, T., Goto, T., Matsunaga, T., Hiyama, E., Hayashi, Y., Ando, H., Suita, S., Kaneko, M., Sakaki, F., Hashizume, K., Ohnuma, N., and Nakagawara, A. (2004) *Oncogene*, in press.

Cisplatin Treatment Induces Down-regulation of Plk1 in Association with Up-regulation of p53 in SH-SY5Y Cells—To analyze whether Plk1 expression could be modulated during the cisplatin-induced apoptosis, whole cell lysates and total RNA were prepared from human neuroblastoma-derived SH-SY5Y cells after treatment with or without cisplatin, and were subjected to immunoblot analysis and RT-PCR, respectively. In accordance with our previous observations (39), cells underwent apoptosis in a time-dependent manner as measured by the cell survival assay (Fig. 2*A*), and a remarkable stabilization of p53 at the protein level was detected after treating the cells with cisplatin, accompanied with a significant up-regulation of p21^{WAF1} both at protein and mRNA levels (Fig. 2, *B* and *C*). In addition to the increase in the level of total p53, the phosphorylation of p53 at Ser^{15} was dramatically enhanced in cells exposed to cisplatin, whereas that of p53 at Ser^{20} was undetectable (data not shown). Intriguingly, cisplatin treatment markedly reduced the expression level of *Plk1* mRNA and protein (Fig. 2, *B* and *C*), suggesting that there exists an inverse relationship between the expression levels of p53 and Plk1 during DNA damage-induced apoptosis. Thus, Plk1 may play an important role in the p53 pathway. On the other hand, cisplatin treatment resulted in a significant up-regulation of *Plk3* mRNA expression in a time-dependent manner, however,

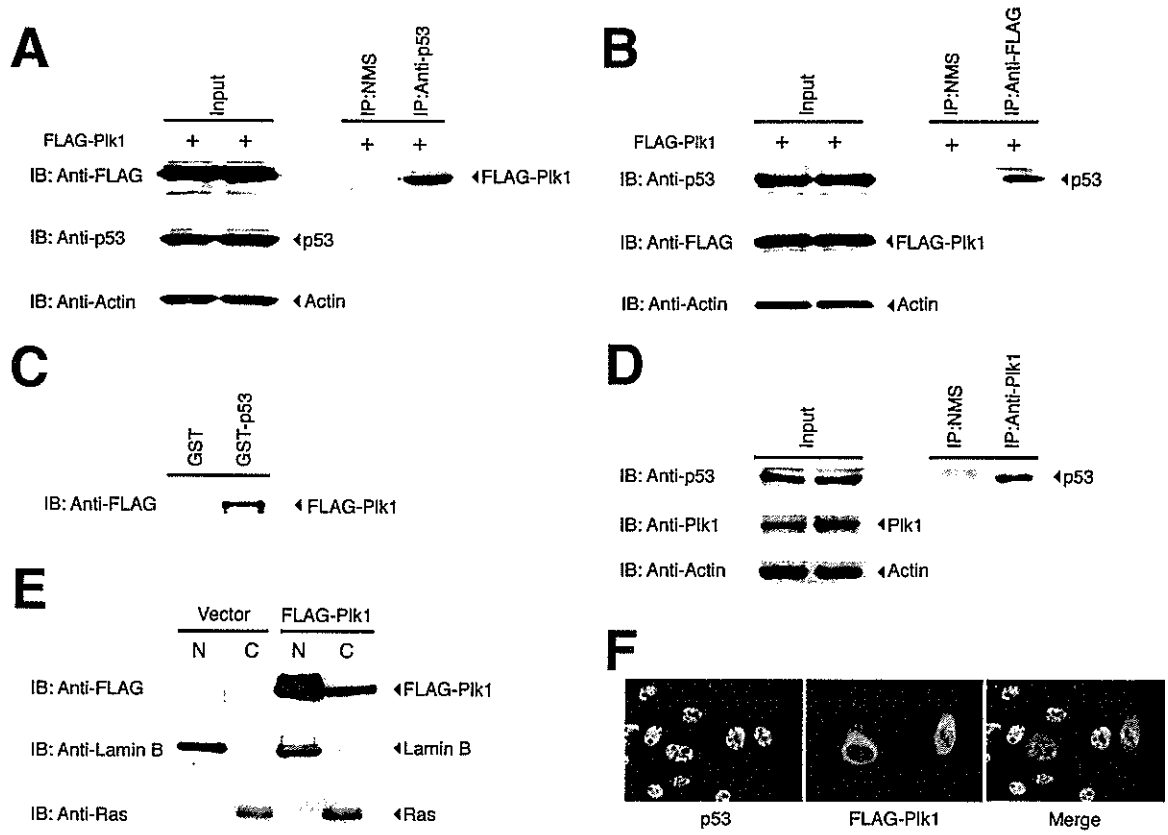

FIG. 3. **Co-immunoprecipitation and nuclear co-localization of Plk1 and p53.** *A*, complex formation between Plk1 and p53 in mammalian cultured cells. COS7 cells were transiently transfected with the expression plasmid for FLAG-tagged Plk1. Forty-eight hours after transfection, whole cell lysates were prepared and immunoprecipitated (*IP*) with NMS or with monoclonal anti-p53 antibodies. The immunocomplexes were resolved by 10% SDS-polyacrylamide gel electrophoresis and immunoblotted (*IB*) with monoclonal anti-FLAG antibody. Whole cell lysates were immunoblotted with monoclonal anti-p53, or with monoclonal anti-FLAG antibody to show the expression of endogenous p53, or FLAG-Plk1, respectively. The p53 blot was reprobed for actin to ensure equal loading. *B*, a similar immunoprecipitation assay was performed with NMS or monoclonal anti-FLAG antibody, followed by immunoblotting with monoclonal anti-p53 antibody. Whole cell lysates were monitored on immunoblot for the expression of endogenous p53 or FLAG-Plk1. The p53 blot was reprobed for actin to ensure equal loading. *C*, GST pull-down assay. Whole cell lysates prepared from COS7 cells expressing FLAG-Plk1 were incubated with GST or GST-p53 immobilized on glutathione-Sepharose beads. The bound proteins were separated by 10% SDS-polyacrylamide gel electrophoresis, and subjected to immunoblotting with the anti-FLAG antibody. *D*, association between endogenous p53 and Plk1. Cell lysates prepared from U2OS cells were immunoprecipitated with NMS or with monoclonal anti-Plk1 antibody, and the anti-Plk1 immunoprecipitates were immunoblotted with monoclonal anti-p53 antibody. *E*, subcellular localization of Plk1. COS7 cells were transiently transfected with the expression plasmid encoding FLAG-Plk1. Forty-eight hours after transfection, cells were fractionated into nuclear (*N*) and cytosolic (*C*) fractions as described under "Experimental Procedures." Equal amounts of each fraction were resolved by 10% SDS-polyacrylamide gel electrophoresis and immunoblotted with monoclonal anti-FLAG antibody (*top panel*). These extracts were also immunoblotted with monoclonal antibody specific for lamin B (*middle panel*) or Ras (RASK-3) (*bottom panel*) to show the validity of our fractionation technique. *F*, nuclear co-localization of Plk1 and p53. COS7 cells were transiently transfected with the FLAG-Plk1 expression plasmid. Following transfection, cells were fixed and incubated with polyclonal anti-p53 and monoclonal anti-FLAG antibodies that were revealed by fluorescein isothiocyanate-conjugated anti-rabbit IgG (*green*) and rhodamine-conjugated anti-mouse IgG (*red*), respectively. Merge analysis (*yellow*) showed the nuclear co-localization of Plk1 and p53.

the amount of Plk3 protein remained constant, regardless of cisplatin treatment.

Interaction of Plk1 with p53—Recently, it has been shown that Plk3 interacts with p53 and is directly involved in the stress-induced phosphorylation of p53 on the serine 20 residue (25, 26, 36, 37). Of note, Xie *et al.* (26) found that Plk1 is able to phosphorylate p53 *in vitro*, however, its functional significance *in vivo* remains unclear. These observations prompted us to investigate possible interactions between Plk1 and p53. For this purpose, COS7 cells, which express a large amount of endogenous p53 (40), were transiently transfected with the expression plasmid for FLAG-tagged Plk1. Whole cell lysates prepared from the transfected cells were immunoprecipitated with NMS or with a monoclonal anti-p53 antibody, and the immunoprecipitates were analyzed by immunoblotting with a monoclonal anti-FLAG antibody. As shown in Fig. 3*A*, FLAG-Plk1 was co-immunoprecipitated with the endogenous p53, but not present in the control immunoprecipitates obtained with the normal mouse serum. The expression of FLAG-Plk1 and the endogenous p53 was confirmed by immunoblot analysis with the antibody against the FLAG epitope and p53, respectively (Fig. 3*A*). Analysis of the anti-FLAG immunoprecipitates also revealed that p53 is co-immunoprecipitated with FLAG-Plk1 (Fig. 3*B*). To confirm their interaction *in vitro*, GST pull-down experiments were performed using GST fusion full-length human p53. As shown in Fig. 3*C*, mammalian expressed FLAG-Plk1 bound to GST-p53 but not to GST alone. Their interaction was further examined using endogenous materials. Whole cell lysates prepared from U2OS cells that carry wild-type p53 (41) were immunoprecipitated with a monoclonal anti-Plk1 antibody and the anti-Plk1 immunoprecipitates were analyzed for the presence of the endogenous p53. As shown in Fig. 3*D*, the endogenous p53 was co-immunoprecipitated with the endogenous Plk1. Similar results were also obtained in HeLa cells (data not shown). These results clearly demonstrate that Plk1 interacts with p53 in mammalian cultured cells and *in vitro*.

To evaluate the subcellular localization of Plk1, we per-

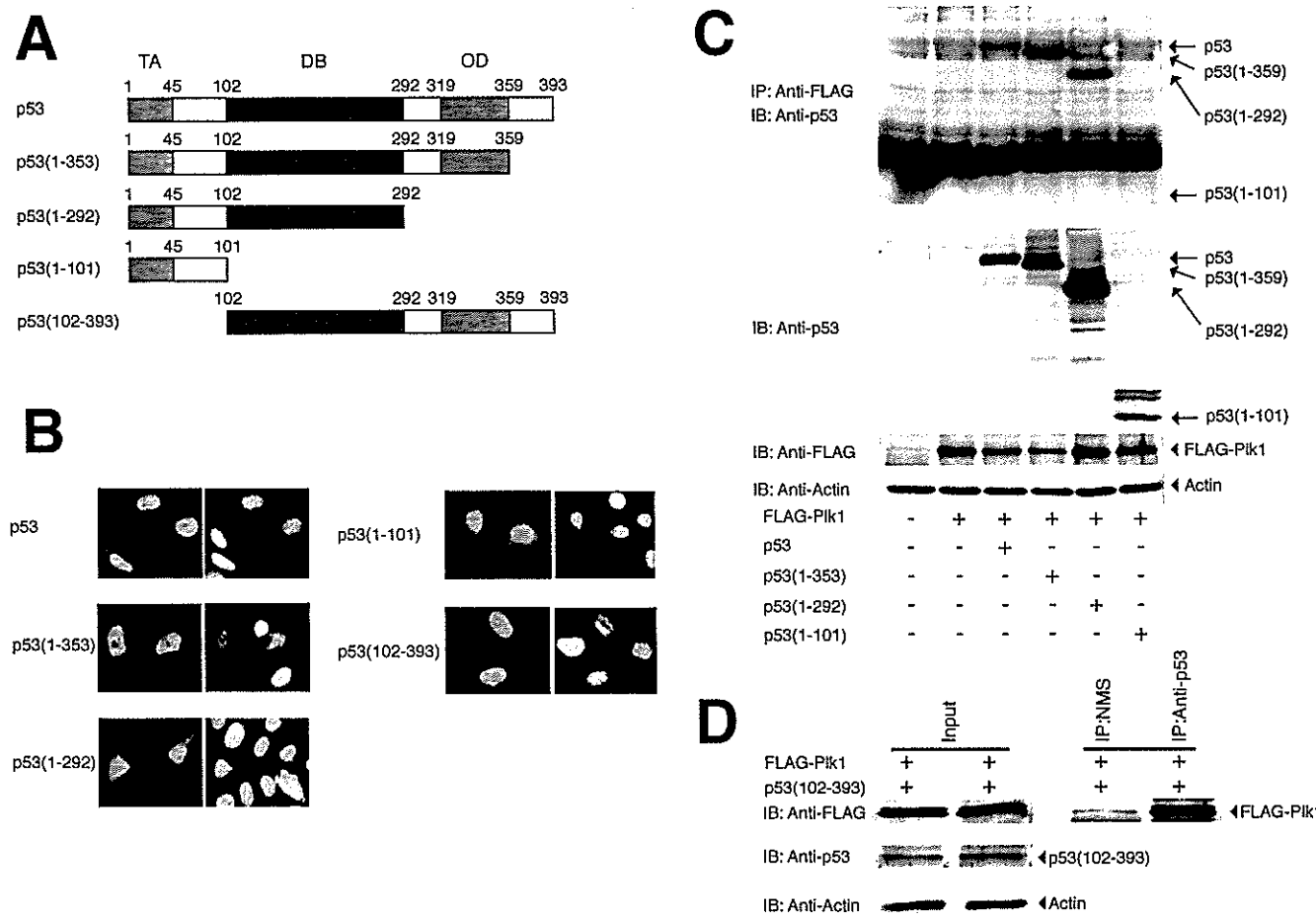

FIG. 4. **DNA-binding domain of p53 is required for interaction with Plk1.** *A*, schematic drawing of full-length p53 and various deletion mutants used in this study. *TA*, transactivation domain; *DB*, sequence-specific DNA-binding domain; *OD*, oligomerization domain. *Numbers* indicate amino acid position. *B*, subcellular localization of various deletion mutants of p53. *p53*-deficient H1299 cells were transiently transfected with the indicated expression plasmids. Forty-eight hours after transfection, cells were fixed and incubated with monoclonal anti-p53 antibody (DO-1 or PAb 421). Cell nuclei were stained with 4,6-diamidino-2-phenylindole (*blue*). Expression of p53 derivatives was visualized with rhodamine-conjugated secondary antibody (*red*). *C* and *D*, Plk1 interacts with the DNA-binding domain of p53. H1299 cells were transiently co-transfected with the indicated combinations of the expression plasmids. Forty-eight hours after transfection, whole cell lysates were prepared and subjected to immunoprecipitation with monoclonal anti-FLAG antibody followed by immunoblotting with monoclonal anti-p53 antibody (*upper panel*). The *lower panels* show the direct immunoblot analyses of whole cell lysates performed with monoclonal anti-p53, monoclonal anti-FLAG, or with polyclonal anti-actin antibody (*C*). Whole cell lysates from H1299 cells overexpressing FLAG-Plk1 and p53-(102–393) were immunoprecipitated with monoclonal anti-p53 antibody (PAb421) or with NMS followed by immunoblotting with monoclonal anti-FLAG antibody. Expression levels of p53-(102–393), FLAG-Plk1, and actin were examined by immunoblotting (*D*).

formed indirect immunofluorescent staining as well as biochemical cell fractionation of the transfected COS7 cells. COS7 cells transfected with the empty plasmid or with the expression plasmid for FLAG-Plk1 were fractionated into cytoplasmic and nuclear fractions for immunoblot analysis of FLAG-Plk1. Ras and lamin B served as markers for the purity of cytoplasmic and nuclear fractions, respectively (Fig. 3*E*, *lower panels*). Consistent with previous observations (10, 22, 42), FLAG-Plk1 was detected both in the cytoplasm and nucleus (Fig. 3*E*, *upper panel*). For immunofluorescent staining, COS7 cells expressing FLAG-Plk1 were fixed and stained with monoclonal anti-FLAG and polyclonal anti-p53 antibodies. As shown in Fig. 3*F*, FLAG-Plk1 localized to both the cytoplasm and nucleus. Merging analysis by confocal microscopy showed that FLAG-Plk1 co-localizes with endogenous p53 in cell nucleus.

The Sequence-specific DNA-binding Region of p53 Is Required for the Interaction with Plk1—To assess regions of p53 involved in the interaction with Plk1, we constructed a series of p53 deletion mutants including p53-(1–359) (lacking an extreme COOH-terminal region), p53-(1–292) (lacking the most COOH-terminal region including an oligomerization domain), p53-(1–101) (retaining only an NH_2-terminal transactivation domain), and p53-(102–393) (lacking an NH_2-terminal transactivation domain) (Fig. 4*A*). We first examined their subcellular localization by indirect immunofluorescent staining. To this end, p53-deficient human lung carcinoma H1299 cells (43) were transiently transfected with each expression plasmid. Forty-eight hours after transfection, cells were fixed and stained with the appropriate monoclonal anti-p53 antibody. As described previously (44, 45), there exist three potential nuclear localization signals (NLS I, II, and III) in the COOH-terminal region of p53, and NLS I alone has an ability to translocate the pyruvate kinase fusion protein to the nucleus. As shown in Fig. 4*B*, wild-type p53 and p53-(102–393), which retain the intact COOH-terminal region, accumulated in the nucleus. In addition, p53-(1–359), which lacks the NLS II and III but retains the NLS I, localized largely in the nucleus. On the other hand, p53-(1–292) and p53-(1–101), which lack three potential NLSs, were detected both in the nucleus and the cytoplasm. We then examined their abilities to interact with Plk1. H1299 cells were transiently co-transfected with the FLAG-Plk1 expression plasmid along with the expression plasmid for wild-type p53, p53-(1–359), p53-(1–292), or p53-(1–101), and the anti-FLAG immunoprecipitates were analyzed for the presence of wild-

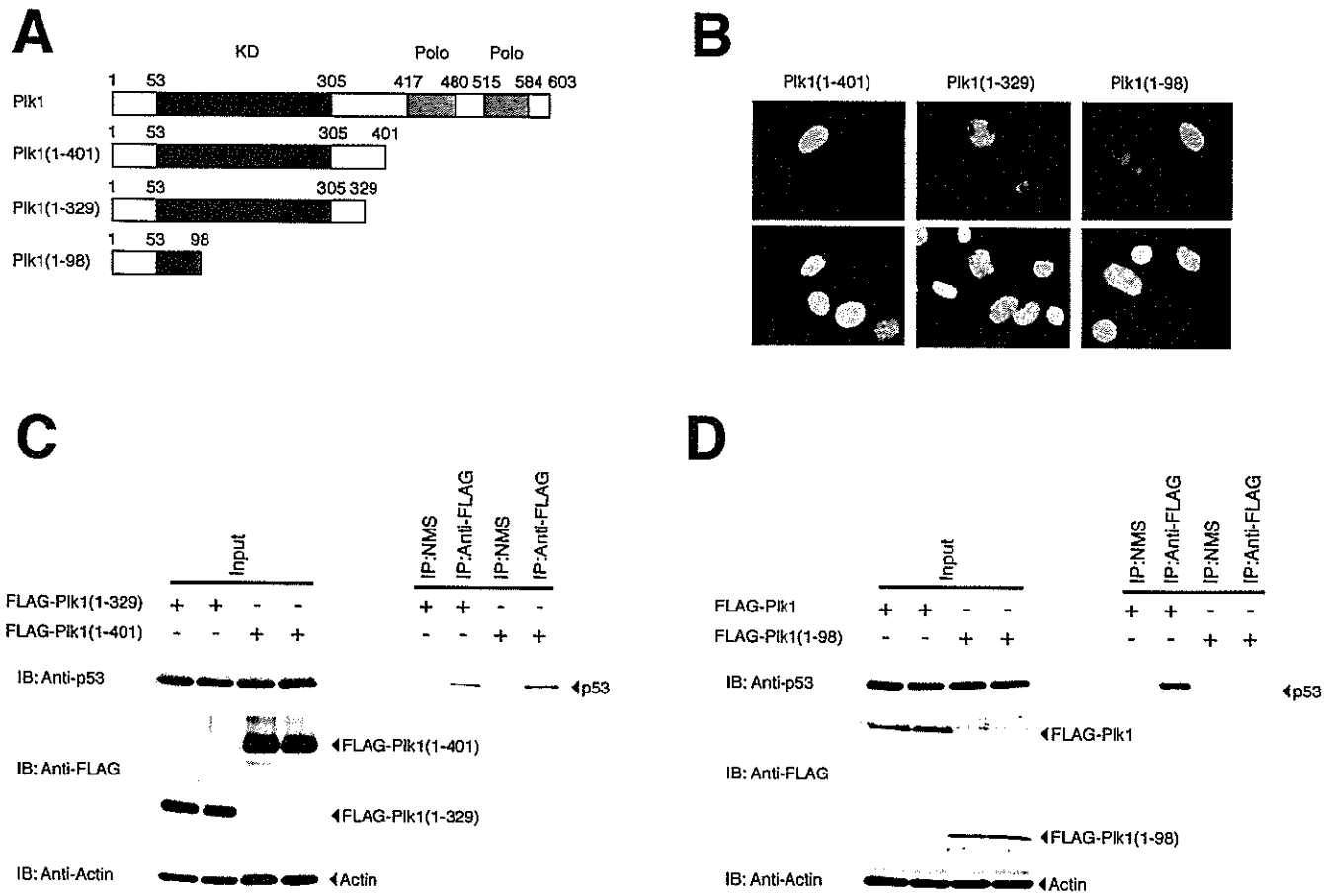

FIG. 5. **Mapping of the region of Plk1 required for interaction with p53.** *A*, schematic representation of Plk1 deletion mutants. *KD*, kinase domain; *Polo*, polo-box. *Numbers* indicate amino acid position. *B*, immunofluorescent studies of Plk1 deletion mutants. Transfected COS7 cells were fixed in 3.7% formaldehyde for 30 min, permeabilized with 0.2% Triton X-100 for 5 min, and blocked in PBS containing 3% bovine serum albumin for 1 h. Cells were then incubated with monoclonal anti-FLAG antibody followed by incubation with rhodamine-conjugated secondary antibody (*red*), and analyzed by confocal microscopy. Cell nuclei were stained with 4,6-diamidino-2-phenylindole (*blue*). *C* and *D*, interaction between various Plk1 deletion mutants and endogenous p53. Whole cell lysates from COS7 cells transfected with the indicated expression plasmids were immunoprecipitated with monoclonal anti-FLAG antibody, and immunoblotted with monoclonal anti-p53 antibody to observe the interaction between Plk1 deletion mutants and p53. Immunoprecipitation with NMS was used as a negative control. Equal amounts of protein derived from cell lysates were immunoblotted with monoclonal anti-p53, monoclonal anti-FLAG, or polyclonal anti-actin antibody.

type p53 and these truncated forms of p53. As shown in Fig. 4*C*, wild-type p53 as well as p53 deletion mutants including p53-(1–359) and p53-(1–292), were detected in the anti-FLAG immunoprecipitates, whereas p53-(1–101) has lost the ability to bind to Plk1, indicating that the extreme COOH-terminal region, the oligomerization domain, and the NH_2-terminal transactivation domain of p53 are not involved in the interaction with Plk1. Similar immunoprecipitation analyses revealed that p53-(102–393) co-precipitates with FLAG-Plk1 (Fig. 4*D*). Thus, the region between amino acid residues 102 and 292 of p53, which includes the sequence-specific DNA-binding domain, appears to be required and sufficient for the interaction with Plk1.

Mapping of the p53-binding Region of Plk1—To map the p53-interacting domain on Plk1, we have constructed the FLAG-tagged Plk1 deletion mutants including Plk1-(1–401), Plk1-(1–329), and Plk1-(1–98) (Fig. 5*A*), and examined their subcellular localization by indirect immunofluorescent staining. As shown in Fig. 5*B*, COS7 cells transfected with each of the expression plasmids for FLAG-tagged Plk1 deletion mutants exhibited intense staining of the nucleus. Inspection of the amino acid sequence of Plk1-(1–98) identified one cluster of basic amino acids (^{48}RSRRRYVRGR^{57}), suggesting that this basic cluster acts as a nuclear localization signal. We then tested the interaction between p53 and each of these Plk1 deletion mutants. COS7 cells were transfected with the expression plasmid encoding Plk1-(1–401), Plk1-(1–329), or Plk1-(1–98), and co-immunoprecipitation experiments were performed to determine the interaction. We found that Plk1-(1–401) and Plk1-(1–329) retained the ability to bind to p53, whereas Plk1-(1–98) did not (Fig. 5*C*). These results indicate that the amino acid sequence comprising residues 99 to 329 of Plk1 contains the p53-binding domain.

Plk1 Inhibits the p53-mediated Transcriptional Activation—To determine whether Plk1 could affect the transcriptional activity of p53, H1299 cells were transiently co-transfected with a constant amount of the expression plasmid encoding p53 together with the p53-responsive *p21^{WAF1}*, *MDM2*, or *BAX*-luciferase reporter constructs in the presence or absence of increasing amounts of the expression plasmid for FLAG-Plk1. Under our experimental conditions, ectopically expressed p53 successfully activated the transcription of each of those p53-responsive reporters as compared with the empty plasmid controls, but Plk1 alone had no effect on luciferase activity (Fig. 6). Expression of FLAG-Plk1 greatly reduced the ability of p53 to increase the *p21^{WAF1}*-, *MDM2*-, and *BAX*-luciferase activities in a dose-dependent manner (Fig. 6, *A–C*). In addition, Plk1-(1–98), which lacks an ability to interact with p53, did not affect the p53 transcriptional activity toward the *p21^{WAF1}*, *MDM2*, and *BAX* promoters (data not shown). To confirm the inhibitory role of Plk1 in the p53-mediated transactivation, we assayed H1299 cell transfectants for induction of the endoge-

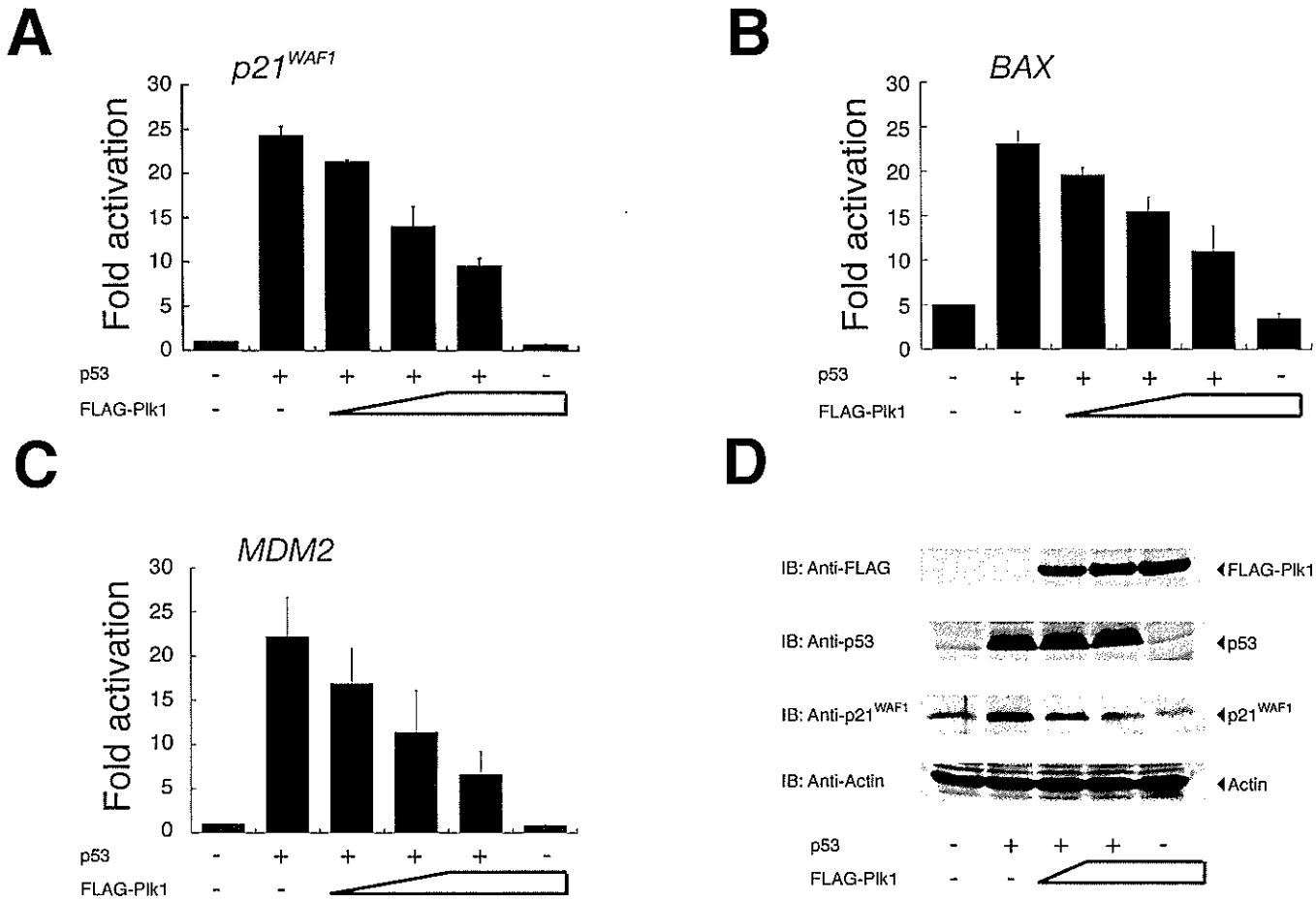

FIG. 6. **Plk1 abrogates the p53-mediated transcriptional activation.** *p53*-deficient H1299 cells (5×10^4 cells/well) were transiently co-transfected with 25 ng of the expression plasmid for p53 together with 100 ng of the luciferase reporter construct that carries the p53-responsive element derived from $p21^{WAF1}$ (*A*), *BAX* (*B*), or *MDM2* (*C*) promoter and 10 ng of the *Renilla* luciferase plasmid (pRL-TK) in the presence or absence of increasing amounts of pcDNA3-FLAG-Plk1 (50, 100, or 200 ng). The total amount of plasmid DNA per transfection was kept constant (510 ng) with pcDNA3. All transfections were performed in triplicate. Forty-eight hours after transfection, cells were lysed, and analyzed for their luciferase activities. Firefly luminescence signal was normalized based on the *Renilla* luminescence signal. Results are shown as -fold induction of the firefly luciferase activity compared with control cells transfected with pcDNA3 alone. *D*, immunoblot analysis. H1299 cells were transiently co-transfected with the indicated combinations of expression plasmids. Whole cell lysates were prepared 48 h post-transfection, and analyzed for the expression of FLAG-Plk1 (*1st panel*), p53 (*2nd panel*), or $p21^{WAF1}$ (*3rd panel*) by immunoblot analysis with monoclonal anti-FLAG, monoclonal anti-p53, or polyclonal anti-$p21^{WAF1}$ antibody, respectively. Total protein levels were controlled with polyclonal anti-actin antibody (*4th panel*).

nous $p21^{WAF1}$. To this end, H1299 cells were transiently co-transfected with a constant amount of the expression plasmid for p53 together with or without increasing amounts of the FLAG-Plk1 expression plasmid. Forty-eight hours after transfection, whole cell lysates were prepared and subjected to immunoblot analysis. Equal protein loading was confirmed by immunoblotting with the antibody against actin. As described (46), overexpression of p53 in H1299 cells resulted in the induction of the endogenous $p21^{WAF1}$ compared with basal levels seen with empty plasmid (Fig. 6*D*, *first* and *second lanes*). Co-expression of p53 with FLAG-Plk1 caused a significant decrease in the endogenous $p21^{WAF1}$ level in a dose-dependent manner (Fig. 6*D*, *third* and *fourth lanes*). These findings strongly suggest that Plk1 has an ability to inhibit p53-mediated transcriptional activation through physical interaction with p53.

To assess the possible effect of the endogenous Plk1 on the transcriptional activity of p53, we have employed an antisense strategy. As shown in Fig. 7*A*, expression of antisense *Plk1* in H1299 cells resulted in a reduction of the endogenous Plk1 as detected by immunoblot analysis. We then performed luciferase reporter analysis utilizing H1299 cells. As expected, co-expression of p53 with the antisense *Plk1* led to a slight but significant increase in the p53-mediated transcriptional activation as compared with cells expressing p53 alone (Fig. 7, *B–D*).

Plk1 Inhibits the p53-mediated Apoptosis—To extend the functional significance of the physical interaction between Plk1 and p53, we next determined whether Plk1 could affect p53-mediated apoptosis. H1299 cells were transiently co-transfected with the expression plasmid encoding p53 together with or without the expression plasmid for FLAG-Plk1. Forty-eight hours after transfection, cell viability was monitored by a cell survival assay. As shown in Fig. 8*A*, overexpression of p53 resulted in a reduction of the number of viable cells as compared with that found in the control transfection, and Plk1 alone had little effect on cell viability. The reduced number of viable cells caused by exogenous p53 was recovered by co-expression of FLAG-Plk1. Considering that p53 induced apoptosis in transfected H1299 cells (47), Plk1 might abrogate the pro-apoptotic function of p53. To confirm this possibility, H1299 cells were transiently co-transfected with a constant amount of the GFP expression plasmid together with the indicated combinations of the expression plasmids. Forty-eight hours after transfection, transfected cells were scored by fluorescence microscopy for the appearance of green fluorescence,

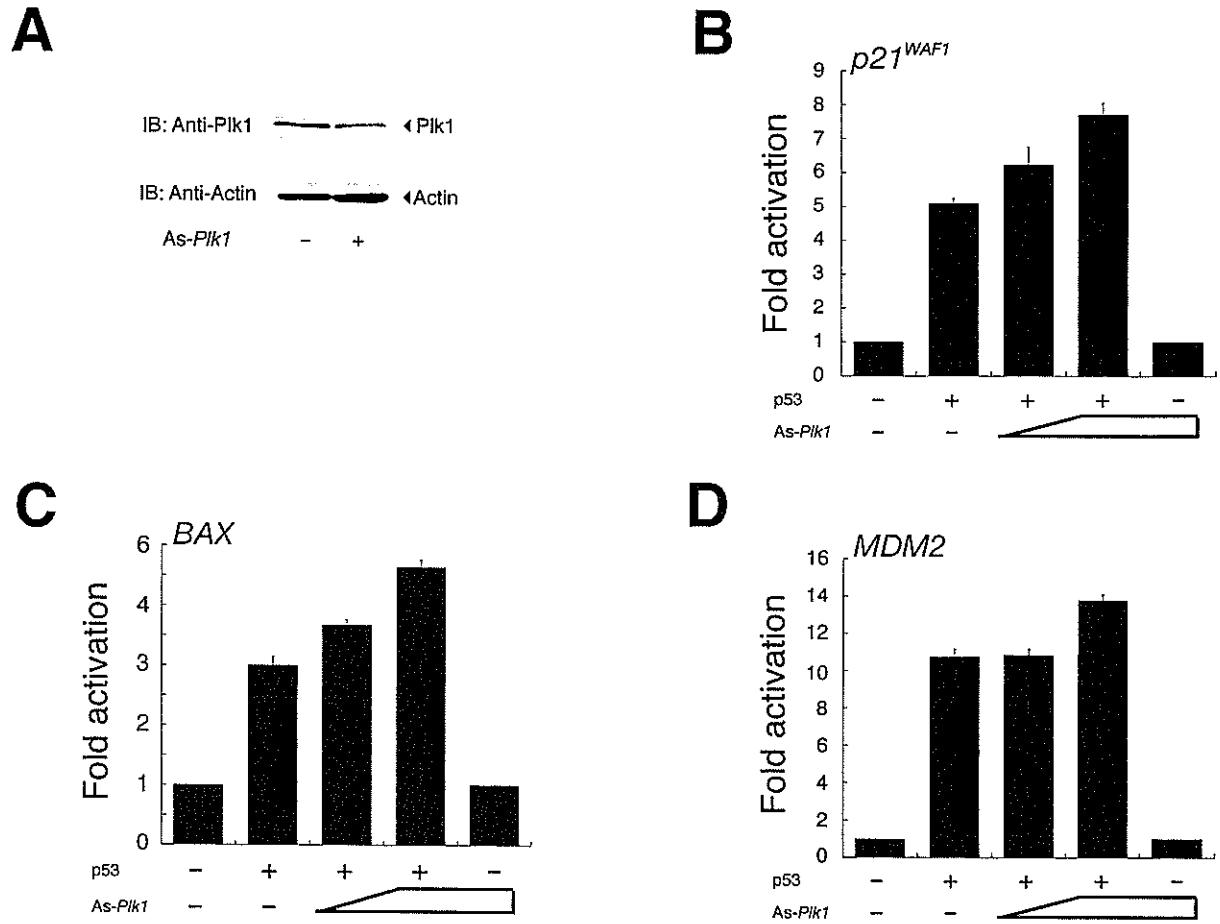

FIG. 7. **Antisense *Plk1* increases the transcriptional activity of p53.** *A*, antisense *Plk1* expression in H1299 cells results in a reduction of endogenous Plk1. H1299 cells were transfected with 2 μg of antisense *Plk1* expression plasmid (*As-Plk1*). Whole cell lysates prepared from transfected cells were subjected to immunoblotting with the anti-Plk1 antibody (*top panel*). Western blotting for actin is shown as a control for protein loading (*bottom panel*). *B–D*, luciferase reporter analysis. H1299 cells were transiently co-transfected with 12.5 ng of the p53 expression plasmid along with 100 ng of the indicated luciferase reporter construct in the presence or absence of increasing amounts of As-*Plk1* (200 and 400 ng). Determination and calculation of the luciferase activities are described in the legend to Fig. 6.

and the number of GFP-positive cells with condensed and fragmented nuclei were counted. Under our experimental conditions, enforced expression of p53 led to an increase in the number of apoptotic cells as compared with the control transfection (Fig. 8*B*). In agreement with the above cell survival assay, co-expression of p53 with FLAG-Plk1 decreased the number of apoptotic cells as compared with that resulting from expression of p53 alone. Taken together, these results indicate that Plk1 is an efficient inhibitor of p53.

Kinase-deficient Plk1 Fails to Inhibit p53—Next, we tested whether the Plk1 kinase activity could be required for Plk1-dependent inhibition of the p53 transcriptional activity. As described previously (22), the mutant form of Plk1 (Plk1-K82M), in which Lys^{82} within the ATP-binding motif is replaced by Met, completely lost the kinase activity. We therefore generated an expression plasmid encoding FLAG-Plk1(K82M), and then examined whether Plk1(K82M) could associate with p53, and also affect the p53-mediated transcriptional activation. Immunoprecipitation followed by Western detection of endogenous p53 indicated that p53 interacted with both the wild-type Plk1 and the kinase-deficient Plk1(K82M) (Fig. 9*A*). The effects of the lysine mutation on the p53-mediated transcriptional activation were tested by luciferase reporter analysis. In contrast to the wild-type Plk1, the kinase-deficient Plk1(K82M) failed to reduce the p53-mediated reporter expression driven by those constructs (Fig. 9, *B–D*).

To examine the effect of Plk1(K82M) on p53-dependent apoptosis, H1299 cells were transfected with the expression plasmid for p53 along with or without the expression plasmid for FLAG-Plk1(K82M). Forty-eight hours after transfection, their viability was measured by cell survival assay. As expected, the p53-dependent decrease in the number of viable cells was unaffected in the presence of the exogenous FLAG-Plk1(K82M) (Fig. 9*E*). Taken together, our results strongly suggest that the kinase activity of Plk1 is required for Plk1-dependent inhibition of p53.

ATM Antagonizes the Inhibitory Effect of Plk1 on p53—Plk1 kinase activity has been shown to be inhibited in an ATM-dependent manner in response to DNA damage (19, 20). The kinase activity of ATM was significantly increased after DNA damage, and ATM was able to phosphorylate p53 at the NH_2 terminus on serine 15 to enhance its stability as well as its transactivation activity (48–50). To examine whether ATM could affect the Plk1-mediated inhibition of p53, we transiently co-transfected H1299 cells with expression plasmids for p53 and FLAG-Plk1 together with or without increasing amounts of ATM expression plasmid, and the ability of p53 to drive transcription from the $p21^{WAF1}$ reporter was measured. As expected, co-expression of p53 with ATM resulted in an increase in the transcriptional activity of p53 as compared with that of cells expressing p53 alone (Fig. 10). Increasing amounts of ATM largely abrogated the Plk1-mediated inhibition of the p53-dependent transcriptional activation. It thus appears that ATM could inhibit the activity of Plk1 and thereby restore the transcriptional activity of p53.

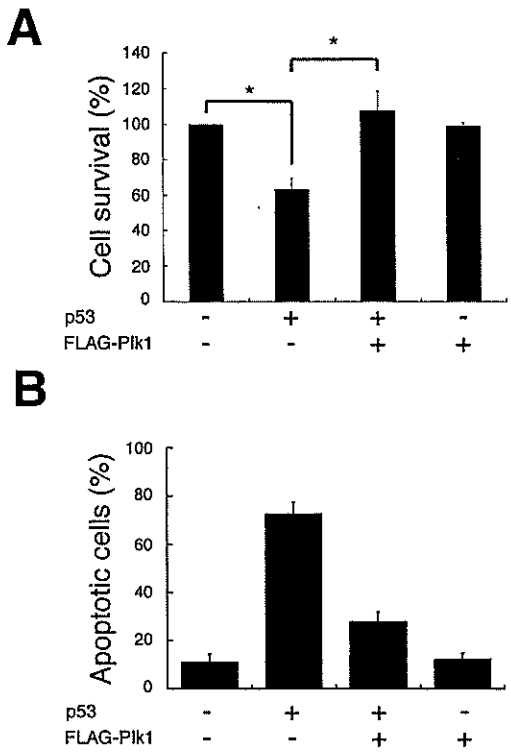

FIG. 8. **Plk1 inhibits the pro-apoptotic activity of p53.** *A*, H1299 cells were transiently co-transfected with 0.6 μg of the expression plasmid for p53 together with or without 1.2 μg of the FLAG-Plk1 expression plasmid. The total amount of plasmid DNA was kept constant (2 μg) with the empty plasmid. At 48 h after transfection, cell viability was determined by MTT cell survival assays. The graph (mean ± S.D. of three independent experiments) represents relative viability based on the percent of viable cells compared with the control transfection (pcDNA3). The percentage of viable cells expressing p53 alone is significantly different from that of viable cells expressing p53 and FLAG-Plk1 ($p < 0.0001$). *B*, H1299 cells were transiently co-transfected with the indicated combinations of the expression plasmids. A constant amount of the GFP expression plasmid (200 ng) was included in all combinations, and the total amount of plasmid DNA was kept constant (2 μg) by including an appropriate amount of empty plasmid. Forty-eight hours after transfection, transfected cells were identified by the presence of green fluorescence. Cell nucleus was stained with propidium iodide to reveal nuclear condensation and fragmentation. The number of GFP-positive cells with condensed and fragmented nuclei was scored, and the percentage of apoptotic cells shown in each column represents the mean of three independent experiments.

DISCUSSION

In the present study, we have found that Plk1 interacts with p53 and inhibits its transactivation as well as apoptosis-inducing activity in mammalian cultured cells. This interaction is mediated by the sequence-specific DNA-binding domain of p53 and the region of Plk1 containing the kinase domain. Importantly, Plk1-mediated inhibition of p53 requires its kinase activity and is attenuated with ATM. Thus, our present data support the hypothesis that p53 is one of the critical targets of Plk1, and that Plk1-mediated inhibition of p53 contributes at least in part to cell fate decisions regarding survival and tumorigenesis.

The expression of *Plk1* was significantly down-regulated in response to cisplatin treatment. Recently, Ree *et al.* (51) found that ionizing radiation leads to the suppression of *Plk1* mRNA expression. It is of interest to examine whether genotoxic stresses other than cisplatin and ionizing radiation could also repress the expression of *Plk1*. On the other hand, *Plk1* mRNA expression is significantly induced in various human primary tumors (27). It is necessary to identify the promoter region as well as the transcription factor(s) required for the transcriptional regulation of *Plk1* in cancerous cells. In good agreement with the previous observations (52), Uchiumi *et al.* (53) have identified the regulatory regions responsible for the activation of the human *Plk1* promoter, which include a consensus Sp1-binding site and a CCAAT box. It has been shown that the transcription factor NF-Y, a heterotrimeric complex consisting of NF-YA, NF-YB, and NF-YC, recognizes and binds to the CCAAT box (54). Indeed, the electrophoretic mobility shift assay revealed that NF-Y binds to the CCAAT box present within the human *Plk1* promoter region, however, it remains to be determined whether NF-Y and/or Sp1 could actually transactivate the *Plk1* promoter in tumor cells (53). Recently, Lee and Pedersen (55) have reported that there exist 6 GC boxes and the CCAAT box within the *type II hexokinase* (*HKII*) promoter, and that NF-Y and Sp family members including Sp1 might contribute to up-regulation of the *HKII* gene in tumor cells. Further studies regarding the transcriptional regulation of the *Plk1* gene are necessary to clarify the molecular mechanisms of Plk1-dependent tumorigenesis.

During the DNA damage response, the activity of ATM is significantly increased and is responsible for the rapid phosphorylation of p53 at Ser^{15} (48–50). This ATM-dependent phosphorylation contributes to the increased stability and activity of p53 by facilitating its dissociation from MDM2 (56). In addition, phosphorylation of p53 at Ser^{15} induces its binding to the transcriptional co-activator p300 (57). Recently, it has been shown that Plk1 activity is inhibited in response to DNA damage, and this inhibition occurs in an ATM-dependent manner (19, 20). Our present data demonstrate that the Plk1-mediated inhibition of p53 activity is rescued by the co-expression of ATM, suggesting that, in addition to the ATM-dependent phosphorylation of p53, the activity of p53 may be enhanced at least in part by the ATM-dependent inhibition of Plk1. Intriguingly, Liu and Erikson (33) reported that p53 is significantly stabilized in Plk1-depleted cells. In accordance with their findings, we have shown that the exposure of SH-SY5Y cells to cisplatin leads to a remarkable accumulation of p53, which is strongly associated with a significant down-regulation of the endogenous Plk1 both at mRNA and protein levels, suggesting that Plk1 is closely involved in the regulation of p53 stability and thereby modulates its activity. Under our experimental conditions, however, overexpression of FLAG-Plk1 did not affect the amounts of the endogenous as well as the ectopically expressed p53.

The pro-apoptotic function of p53 involves its ability to act as a transcription factor in transactivating downstream target gene promoters. The majority of missense mutations of p53 detected in human tumors occur within its sequence-specific DNA-binding domain, and these mutations cause the loss of p53 activity (58). Thus, the structural integrity of this domain is required for p53 function. On the other hand, several viral and cellular proteins inactivate p53 through a variety of different mechanisms (58). MDM2 and Pirh2 promote ubiquitination and degradation of p53 (59–62). Sir2α interacts with p53 and induces its deacetylation (63). In addition, S100B calcium-binding protein prevents the oligomerization of p53 to inhibit its function (64). Based on our systematic immunoprecipitation analysis, Plk1 binds to p53 through the sequence-specific DNA-binding domain of p53. Intriguingly, SV40 large T antigen binds to the sequence-specific DNA-binding domain of p53, and abrogates DNA binding as well as the transactivation function of p53 (65, 66). It is thus likely that, like SV40 large T antigen, Plk1 might mask this domain of p53 by direct binding, and thereby inhibit its sequence-specific transcriptional activity. Further study is required to identify the detailed molecular mechanism.

In sharp contrast to Plk1, Xie *et al.* (26) found that the kinase

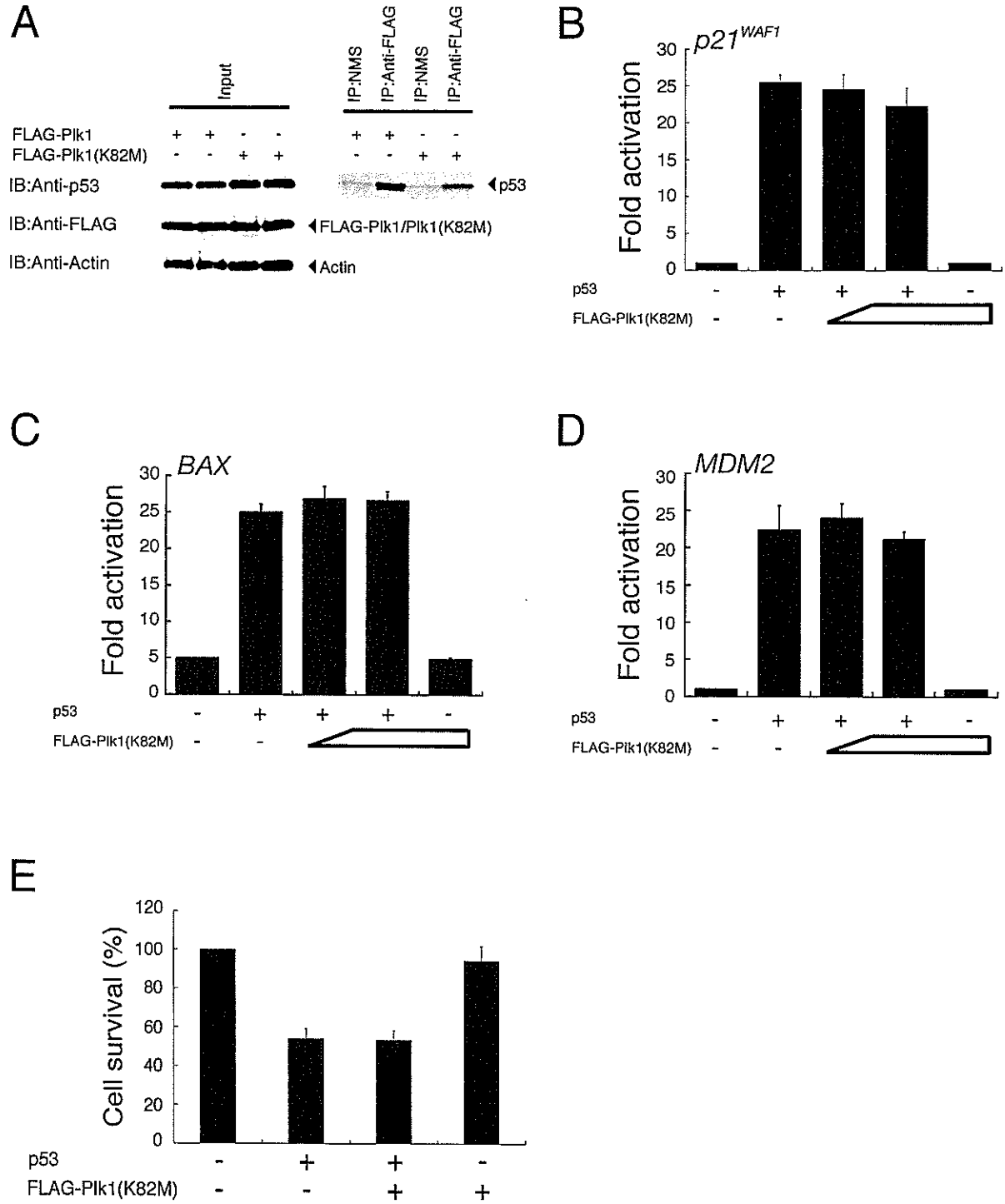

FIG. 9. **Kinase-deficient Plk1(K82M) fails to reduce the activity of p53.** *A*, Plk1(K82M) retains an ability to interact with p53. COS7 cells were transiently transfected with the expression plasmid for FLAG-Plk1 or FLAG-Plk1(K82M). Forty-eight hours after transfection, cell lysates were prepared and subjected to anti-FLAG immunoprecipitation followed by immunoblotting with monoclonal anti-p53 antibody. Immunoprecipitation with NMS was used as a negative control. Equal amounts of protein derived from cell lysates were immunoblotted with monoclonal anti-p53, monoclonal anti-FLAG, or with polyclonal anti-actin antibody. *B–D*, Plk1(K82M) has an undetectable effect on the transcriptional activity of p53. H1299 cells were transiently co-transfected with a fixed amount of the p53 expression plasmid (25 ng) and the p53-responsive luciferase reporter construct carrying the $p21^{WAF1}$ (*B*), *BAX* (*C*), or *MDM2* (*D*) promoter (100 ng) in the presence or absence of increasing amounts of the expression plasmid encoding FLAG-Plk1(K82M) (100 or 200 ng). The total amount of plasmid DNA per transfection was kept constant (510 ng) with pcDNA3. Determination and calculation of the luciferase activities are described in the legend to Fig. 6. *E*, Plk1(K82M) is unable to inhibit the pro-apoptotic function of p53. H1299 cells were transiently co-transfected with the p53 expression plasmid (0.6 μg) together with or without the expression plasmid for FLAG-Plk1(K82M) (1.2 μg). Forty-eight hours after transfection, their viability was measured by MTT cell survival assays as described in the legend to Fig. 8.

activity of Plk3 is rapidly enhanced in response to DNA damage in an ATM-dependent fashion. They also described that Plk3 has the ability to interact directly with p53 and phosphorylate p53 at Ser^{20}. Moreover, a kinase-defective mutant form of Plk3 fails to phosphorylate p53, and abrogates the p53-mediated transcriptional activation as well as growth suppression, indicating that Plk3 might enhance the p53 activity through Ser^{20} phosphorylation of p53 (26). In addition to Ser^{15} phosphoryla-

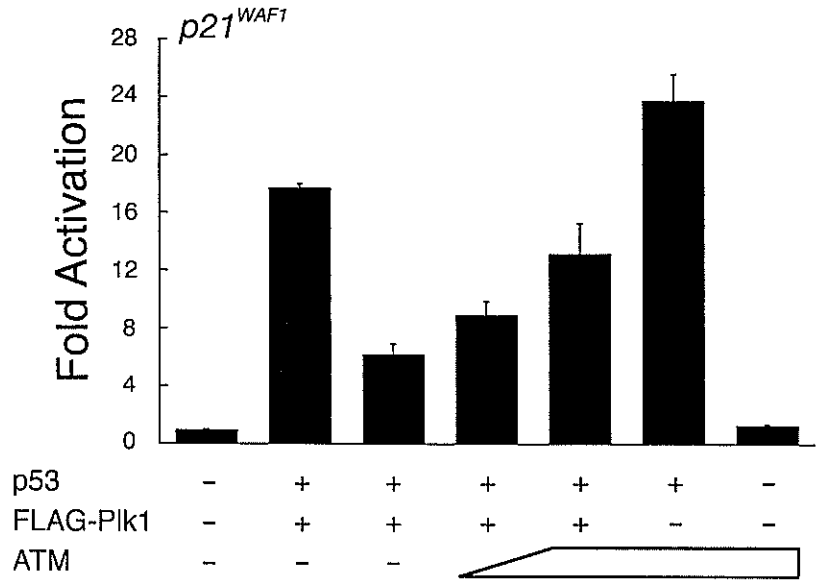

FIG. 10. **ATM antagonizes the inhibitory effect of Plk1 on the p53-dependent transactivation.** H1299 cells were transiently co-transfected with the expression plasmids encoding p53 (25 ng) and FLAG-Plk1 (200 ng) along with the luciferase reporter construct containing the p53-responsive element from the $p21^{WAF1}$ promoter in the presence or absence of increasing amounts of ATM expression plasmid (50 or 100 ng). pcDNA3 was used to equalize the amount of plasmid in each transfection, and the *Renilla* luciferase plasmid was included in the transfection mixture to normalize the transfection efficiency. Determination and calculation of the luciferase activities are described in the legend to Fig. 6.

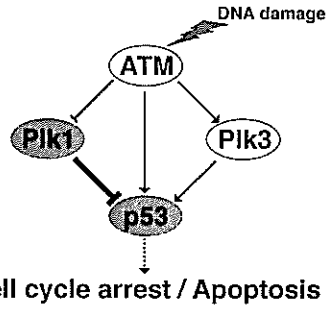

FIG. 11. **Schematic representation of interactions among ATM, Plk1, Plk3, and p53 in response to DNA damage.**

tion of p53, DNA damage-induced phosphorylation of p53 at Ser^{20} prevents its association with MDM2 and results in its stabilization (67). Of note, it has been shown that Plk1 phosphorylates p53 *in vitro* but on residues that might be different from that mediated by Plk3 (26). According to their phosphopeptide mapping analysis, at least three unique radiolabeled tryptic peptides derived from recombinant p53 were detected in the presence of Plk1. Recently, Nakajima *et al.* (68) identified a sequence (D/E)*X*(S/T)ψ*X*(D/E) (*X*, any amino acid; ψ, a hydrophobic amino acid) as a consensus motif for Plk1-dependent phosphorylation (68). During the search for a putative phosphorylation site(s) targeted by Plk1 within the amino acid sequence of p53, we found a related motif (^{254}IITLED^{259}) present within the sequence-specific DNA-binding domain of p53, suggesting that this motif could be one of the putative phosphorylation sites of p53 targeted by Plk1, although there is no direct evidence for this possibility. According to our present results, the kinase-deficient mutant form of Plk1 that retained an ability to associate with p53, failed to reduce the transcriptional as well as apoptosis-inducing activity of p53, suggesting that the kinase activity of Plk1 is critical for the Plk1-dependent inhibition of p53. Thus, identification of the major phosphorylation site(s) of p53 by Plk1 is required to establish the functional significance of the Plk1-mediated phosphorylation of p53. In contrast, Liu and Erikson (33) reported that, like wild-type mouse Plk1, co-expression of the kinase-defective (K82M) mouse Plk1 partially rescued the apoptotic phenotype induced by the depletion of Plk1, indicating that the kinase activity is not necessary for its anti-apoptotic activity. They also described that their kinase-defective mouse Plk1 has 15–20% of wild-type kinase activity, raising a possibility that the residual kinase activity of their mouse Plk1(K82M) might be enough to inhibit the Plk1 depletion-induced apoptosis.

Fig. 11 shows a model that incorporates our present findings, and illustrates various interactions in response to DNA damage. Given the fact that the differential expression of Plk1 and Plk3 during the cisplatin-induced apoptosis, and their differential effects on p53, it is conceivable that the balance between intracellular expression levels of Plk1 with oncogenic potential and pro-apoptotic Plk3 is at least in part responsible for the determination of the cell fate via the physical and functional interaction with p53.

Acknowledgments—We are grateful to Dr. Y. Shiloh and the Japanese Study Group for Pediatric Liver Tumor for kindly providing the ATM expression plasmid and hepatoblastoma tissues, respectively. We thank Dr. S. Sakiyama and members of our laboratory for helpful discussions. We also thank Y. Nakamura and M. Kikawa for excellent technical assistance.

REFERENCES

1. Glover, D. M., Hagan, I. M., and Tavares, A. A. (1998) *Genes Dev.* **12**, 3777–3787
2. Clay, F. J., McEwen, S. J., Bertoncello, I., Wilks, A. F., and Dunn, A. R. (1993) *Proc. Natl. Acad. Sci. U. S. A.* **90**, 4882–4886
3. Lee, K. S., Grenfell, T. Z., Yarm, F. R., and Erikson, R. L. (1998) *Proc. Natl. Acad. Sci. U. S. A.* **95**, 9301–9306
4. Song, S., Grenfell, T., Garfield, S., Erikson, R. L., and Lee, K. S. (2000) *Mol. Cell. Biol.* **20**, 286–298
5. Jang, Y.-J., Lin, C.-Y., Ma, S., and Erikson, R. L. (2002) *Proc. Natl. Acad. Sci. U. S. A.* **99**, 1984–1989
6. Glover, D. M., Ohkura, H., and Tavares, A. (1996) *J. Cell Biol.* **135**, 1681–1684
7. Lane, H., and Nigg, E. A. (1997) *Trends Cell. Biol.* **7**, 63–68
8. Nigg, E. A. (1998) *Curr. Opin. Cell Biol.* **10**, 776–783
9. Hamanaka, R., Maloid, S., Smith, M. R., O'Connell, C. D., Longo, D. L., and Ferris, D. K. (1994) *Cell Growth & Differ.* **5**, 249–257
10. Smith, M. R., Wilson, M. L., Hamanaka, R., Chase, D., Kung, H.-F., Longo, D. L., and Ferris, D. K. (1997) *Biochem. Biophys. Res. Commun.* **234**, 397–405
11. Lake, R. J., and Jelinek, W. R. (1993) *Mol. Cell. Biol.* **13**, 7793–7801
12. Golsteyn, R. M., Schultz, S. J., Bartek, J., Ziemiecki, A., Ried, T., and Nigg, E. A. (1994) *J. Cell Sci.* **107**, 1509–1517
13. Holtrich, U., Wolf, G., Brauninger, A., Karn, T., Bohme, B., Rubsamen-Waigmann, H., and Strebhardt, K. (1994) *Proc. Natl. Acad. Sci. U. S. A.* **91**, 1736–1740
14. Simmons, D. L., Neel, B. G., Stevens, R., Evett, G., and Erikson, R. L. (1992) *Mol. Cell. Biol.* **12**, 4164–4169
15. Donohue, P. J., Alberts, G. F., Guo, Y., and Winkles, J. A. (1995) *J. Biol. Chem.* **270**, 10351–10357
16. Golsteyn, R. M., Mundt, K. E., Fry, A. M., and Nigg, E. A. (1995) *J. Cell Biol.* **129**, 1617–1628
17. Hamanaka, R., Smith, M. R., O'Connor, P. M., Maloid, S., Mihalic, K., Spivak, J. L., Longo, D. L., and Ferris, D. K. (1995) *J. Biol. Chem.* **270**, 21086–21091
18. Qian, Y.-W., Erikson, E., and Maller, J. L. (1998) *Science* **282**, 1701–1704
19. Smits, V. A., Klompmaker, R., Arnaud, L., Rijksen, G., Nigg, E. A., and Medema, R. H. (2000) *Nat. Cell Biol.* **2**, 672–676
20. van Vugt, M. A. T. M., Smits, V. A. J., Klompmaker, R., and Medema, R. H. (2001) *J. Biol. Chem.* **276**, 41656–41660
21. Toyoshima-Morimoto, F., Taniguchi, E., Shinya, N., Iwamatsu, A., and

Nishida, E. (2001) *Nature* **410,** 215–220
22. Yuan, J., Eckerdt, F., Bereiter-Hahn, J., Kurunci-Csacsko, E., Kaufmann, M., and Strebhardt, K. (2002) *Oncogene* **21,** 8282–8292
23. Toyoshima-Morimoto, F., Taniguchi, E., and Nishida, E. (2002) *EMBO Rep.* **3,** 341–348
24. Ouyang, B., Pan, H., Lu, L., Li, J., Stambrook, P., Li, B., and Dai, W. (1997) *J. Biol. Chem.* **272,** 28646–28651
25. Bahassi, E. M., Conn, C. W., Myer, D. L., Hennigan, R. F., McGowan, C. H., Sanchez, Y., and Stambrook, P. J. (2002) *Oncogene* **21,** 6633–6640
26. Xie, S., Wu, H., Wang, Q., Cogswell, J. P., Husain, I., Conn, C., Stambrook, P., Jhanwar-Uniyal, M., and Dai, W. (2001) *J. Biol. Chem.* **276,** 43305–43312
27. Yuan, J., Horlin, A., Hock, B., Stutte, H. J., Rubsamen-Waigmann, H., and Strebhardt, K. (1997) *Am. J. Pathol.* **150,** 1165–1172
28. Wolf, G., Elez, R., Doermer, A., Holtrich, U., Ackermann, H., Stutte, H. J., Altmannsberger, H. M., Rubsamen-Waigmann, H., and Strebhardt, K. (1997) *Oncogene* **14,** 543–549
29. Knecht, R., Elez, R., Oechler, M., Solbach, C., von Ilberg, C., and Strebhardt, K. (1999) *Cancer Res.* **59,** 2794–2797
30. Knecht, R., Oberhauser, C., and Strebhardt, K. (2000) *Int. J. Cancer* **89,** 535–536
31. Spankuch-Schmitt, B., Wolf, G., Solbach, C., Loibl, S., Knecht, R., Stegmuller, M., von Minckwitz, G., Kaufmann, M., and Strebhardt, K. (2002) *Oncogene* **21,** 3162–3171
32. Spankuch-Schmitt, B., Bereiter-Hahn, J., Kaufmann, M., and Strebhardt, K. (2002) *J. Natl. Cancer Inst.* **94,** 1863–1877
33. Liu, X., and Erikson, R. L. (2003) *Proc. Natl. Acad. Sci. U. S. A.* **100,** 5789–5794
34. Li, B., Ouyang, B., Pan, H., Reissmann, P. T., Slamon, D. J., Arceci, R., Lu, L., and Dai, W. (1996) *J. Biol. Chem.* **271,** 19402–19408
35. Dai, W., Li, Y., Ouyang, B., Pan, H., Reissmann, P., Li, J., Wiest, J., Stambrook, P., Gluckman, J. L., Noffsinger, A., and Bejarano, P. (2000) *Genes Chromosomes Cancer* **27,** 332–336
36. Conn, C. W., Hennigan, R. F., Dai, W., Sanchez, Y., and Stambrook, P. J. (2000) *Cancer Res.* **60,** 6826–6831
37. Xie, S., Wang, Q., Wu, H., Cogswell, J., Lu, L., Jhanwar-Uniyal, M., and Dai, W. (2001) *J. Biol. Chem.* **276,** 36194–36199
38. Nakamura, Y., Ozaki, T., Nakagawara, A., and Sakiyama, S. (1997) *Eur. J. Cancer* **33,** 1986–1990
39. Nakagawa, T., Takahashi, M., Ozaki, T., Watanabe, K., Todo, S., Mizuguchi, H., Hayakawa, T., and Nakagawara, A. (2002) *Mol. Cell. Biol.* **22,** 2575–2585
40. Watanabe, K., Ozaki, T., Nakagawa, T., Miyazaki, K., Takahashi, M., Hosoda, M., Hayashi, S., Todo, S., and Nakagawara, A. (2002) *J. Biol. Chem.* **277,** 15113–15123
41. Kim, E.-J., Park, J.-S., and Um, S.-J. (2002) *J. Biol. Chem.* **277,** 32020–32028
42. Taniguchi, E., Totoshima-Morimoto, F., and Nishida, E. (2002) *J. Biol. Chem.* **277,** 48884–48888
43. Kastan, M. B., Zhan, Q., el-Deiry, W. S., Carrier, F., Jacks, T., Walsh, W. V., Plunkett, B. S., Vogelstein, B., and Fornace, A. J., Jr. (1992) *Cell* **71,** 587–597
44. Shaulsky, G., Goldfinger, N., Ben-Ze'ev, A., and Rotter, V. (1990) *Mol. Cell. Biol.* **10,** 6565–6577
45. Dang, C. V., and Lee, W. M. (1989) *J. Biol. Chem.* **264,** 18019–18023
46. Zaika, A. I., Slade, N., Erster, S. H., Sansome, C., Joseph, T. W., Pearl, M., Chalas, E., and Moll, U. M. (2002) *J. Exp. Med.* **196,** 765–780
47. Zeng, X., Chen, L., Jost, C. A., Maya, R., Keller, D., Wang, X., Kaelin, W. G., Oren, M., Chen, J., and Lu, H. (1999) *Mol. Cell. Biol.* **19,** 3257–3266
48. Banin, S., Moyal, L., Shieh, S., Taya, Y., Anderson, C. W., Chessa, L., Smorodinsky, N. I., Prives, C., Reiss, Y., Shiloh, Y., and Ziv, Y. (1998) *Science* **281,** 1674–1677
49. Canman, C. E., Lim, D. S., Cimprich, K. A., Taya, Y., Tamai, K., Sakaguchi, K., Appella, E., Kastan, M. B., and Siliciano, J. D. (1998) *Science* **281,** 1677–1679
50. Khanna, K. K., Keating, K. E., Kozlov, S., Scott, S., Gatei, M., Hobson, K., Taya, Y., Gabrielli, B., Chan, D., Lees Miller, S. P., and Lavin, M. F. (1998) *Nat. Genet.* **20,** 398–400
51. Ree, A. H., Bratland, A., Nome, R. V., Stokke, T., and Fodstad, O. (2003) *Oncogene* **22,** 8952–8955
52. Brauninger, A., Strebhardt, K., and Rubsamen-Waigmann, H. (1995) *Oncogene* **11,** 1793–1800
53. Uchiumi, T., Longo, D. L., and Ferris, D. K. (1997) *J. Biol. Chem.* **272,** 9166–9174
54. Mantovani, R. (1999) *Gene (Amst.)* **239,** 15–27
55. Lee, M. G., and Pedersen, P. L. (2003) *J. Biol. Chem.* **278,** 41047–41058
56. Shieh, S. Y., Ikeda, M., Taya, Y., and Prives, C. (1997) *Cell* **91,** 325–334
57. Lambert, P. F., Kashanchi, F., Radonovich, M. F., Shiekhattar, R., and Brady, J. N. (1998) *J. Biol. Chem.* **273,** 33048–33053
58. Prives, C., and Hall, P. A. (1999) *J. Pathol.* **187,** 112–126
59. Haupt, Y., Maya, R., Kazaz, A., and Oren, M. (1997) *Nature* **387,** 296–299
60. Kubbutat, M. H. G., Jones, S. N., and Vousden, K. H. (1997) *Nature* **387,** 299–303
61. Honda, R., Tanaka, H., and Yasuda, Y. (1997) *FEBS Lett.* **420,** 25–27
62. Leng, R. P., Lin, Y., Ma, W., Wu, H., Lemmers, B., Chung, S., Parant, J. M., Lozano, G., Hakem, R., and Benchimol, S. (2003) *Cell* **112,** 779–791
63. Luo, J., Nikolaev, A. Y., Imai, S., Chen, D., Su, F., Shiloh, A., Guarente, L., and Gu, W. (2001) *Cell* **107,** 137–148
64. Lin, J., Blake, M., Tang, C., Zimmer, D., Rustandi, R. R., Weber, D. J., and Carrier, F. (2001) *J. Biol. Chem.* **276,** 35037–35041
65. Tan, T.-H., Wallis, J., and Levine, A. J. (1986) *J. Virol.* **59,** 574–583
66. Farmer, G., Bargonetti, J., Zhu, H., Friedman, P., Prywes, R., and Prives, C. (1992) *Nature* **358,** 83–86
67. Vousden, K. H. (2002) *Biochim. Biophys. Acta* **1602,** 47–59
68. Nakajima, H., Toyoshima-Morimoto, F., Taniguchi, E., and Nishida, E. (2003) *J. Biol. Chem.* **278,** 25277–25280

Oncogene (2004) 23, 5901–5911

www.nature.com/onc

Expression profiling and differential screening between hepatoblastomas and the corresponding normal livers: identification of high expression of the *PLK1* oncogene as a poor-prognostic indicator of hepatoblastomas

Shin-ichi Yamada[1], Miki Ohira[1], Hiroshi Horie[2], Kiyohiro Ando[1], Hajime Takayasu[1], Yutaka Suzuki[3], Sumio Sugano[3], Takahiro Hirata[4], Takeshi Goto[4], Tadashi Matsunaga[2], Eiso Hiyama[2], Yutaka Hayashi[2], Hisami Ando[2], Sachiyo Suita[2], Michio Kaneko[2], Fumiaki Sasaki[2], Kohei Hashizume[2], Naomi Ohnuma[2] and Akira Nakagawara*[,1,2]

[1]*Division of Biochemistry, Chiba Cancer Center Research Institute, Chiba 260-8717, Japan;* [2]*Japanese Study Group for Pediatric Liver Tumor, Japan;* [3]*Human Genome Center, Institute of Medical Science, University of Tokyo, Tokyo 108-8639, Japan;* [4]*Hisamitsu Pharmaceutical Co. Inc., Tokyo 100-6221, Japan*

Hepatoblastoma is one of the most common malignant liver tumors in young children. Recent evidences have suggested that the abnormalities in Wnt signaling pathway, as seen in frequent mutation of the *β-catenin* gene, may play a role in the genesis of hepatoblastoma. However, the precise mechanism to cause the tumor has been elusive. To identify novel hepatoblastoma-related genes for unveiling the molecular mechanism of the tumorigenesis, a large-scale cloning of cDNAs and differential screening of their expression between hepatoblastomas and the corresponding normal livers were performed. We constructed four full-length-enriched cDNA libraries using an oligo-capping method from the primary tissues which included two hepatoblastomas with high levels of alpha-fetoprotein (AFP), a hepatoblastoma without production of AFP, and a normal liver tissue corresponded to the tumor. Among the 10431 cDNAs randomly picked up and successfully sequenced, 847 (8.1%) were the genes with unknown function. Of interest, the expression profile among the two subsets of hepatoblastoma and a normal liver was extremely different. A semiquantitative RT–PCR analysis showed that 86 out of 1188 genes tested were differentially expressed between hepatoblastomas and the corresponding normal livers, but that only 11 of those were expressed at high levels in the tumors. Notably, *PLK1* oncogene was expressed at very high levels in hepatoblastomas as compared to the normal infant's livers. Quantitative real-time RT–PCR analysis for the *PLK1* mRNA levels in 74 primary hepatoblastomas and 29 corresponding nontumorous livers indicated that the patients with hepatoblastoma with high expression of *PLK1* represented significantly poorer outcome than those with its low expression (5-year survival rate: 55.9 vs 87.0%, respectively, $p = 0.042$), suggesting that the level of *PLK1* expression is a novel marker to predict the prognosis of hepatoblastoma. Thus, the differentially expressed genes we have identified may become a useful tool to develop new diagnostic as well as therapeutic strategies of hepatoblastoma.
Oncogene (2004) **23**, 5901–5911. doi:10.1038/sj.onc.1207782
Published online 28 June 2004

Keywords: hepatoblastoma; expression profile; oligo-capping cDNA library; PLK1; prognostic factor

Introduction

Hepatoblastoma (HBL) is the most common hepatic cancer in children (Exelby *et al.*, 1975; Weinberg and Finegold, 1983). However, the etiology of HBL has been unclear in contrast to the adult hepatocellular carcinoma (HCC), in which preceding infection of hepatitis virus is often found (Buendia, 1992; Idilman *et al.*, 1998). Although most HBLs are sporadic, it is sometimes associated with certain hereditary diseases such as Beckwith–Wiedemann syndrome (Albrecht *et al.*, 1994) and familial adenomatous polyposis (Li *et al.*, 1987; Giardiello *et al.*, 1996; Kinzler and Vogelstein, 1996). In the former, loss of heterozygosity of chromosome 11p15.5 is frequently observed, and the abnormal regulation of the *insulin-like growth factor 2* (*IGF2*) and the *H19* genes at this locus may contribute to the disease (Albrecht *et al.*, 1994; Montagna *et al.*, 1994; Li *et al.*, 1995; Rainier *et al.*, 1995; Yun *et al.*, 1998; Fukuzawa *et al.*, 1999). In the latter, the *APC* gene, which is one of the key molecules in Wnt signaling, was found to be constitutively mutated (Kinzler and Vogelstein, 1996).

Increasing evidence suggests that Wnt signaling pathway also plays an important role in the genesis of sporadic hepatoblastomas. A high frequency (more than 60% in some reports) of somatic mutations in the *β-catenin* gene has recently been reported in sporadic tumors (Koch *et al.*, 1999; Wei *et al.*, 2000; Takayasu

*Correspondence: A Nakagawara, Division of Biochemistry, Chiba Cancer Center Research Institute, 666-2 Nitona, Chiba 260-8717, Japan; E-mail: akiranak@chiba-ccri.chuo.chiba.jp
Received 9 December 2003; revised 26 March 2004; accepted 1 April 2004; published online 28 June 2004

et al., 2001; Buendia, 2002). Mutant β-catenin proteins accumulate in the nucleus, resulting in stimulating transcription of the target genes such as *c-myc* and *cyclin D1* (Morin *et al.*, 1997; Polakis, 1999). Mutation in the *Axin* gene, whose product is an antagonist of nuclear accumulation of β-catenin, has also been found in HBL and may contribute to the pathogenesis of the tumors without *β-catenin* mutation (Taniguchi *et al.*, 2002; Miao *et al.*, 2003). However, the molecular mechanism underlying the pathogenesis of HBL is still largely unknown.

Recent progress in therapeutic strategies including intensive chemotherapy and liver transplantation improved the outcome of the patients with HBL. However, the prognosis of a significant fraction of the tumors still remains poor. The clinical markers currently used for HBL include staging, which is a major instrument for assessing prognosis (Hata, 1990), serum alpha-fetoprotein (AFP) (Mann *et al.*, 1978), mitotic activity (Haas *et al.*, 1989), DNA ploidy (Hata *et al.*, 1991), nuclear localization of β-catenin (Park *et al.*, 2001), p53 mutation (Oda *et al.*, 1995), and chromosomal alteration (Weber *et al.*, 2000). Serum AFP level is used as a diagnostic marker to monitor the tumor progression, responsiveness to the therapy, and recurrence after the treatment. Extremely high levels of serum AFP are reported to be associated with aggressiveness of the tumors with unfavorable outcome (van Tornout *et al.*, 1997), except some reports showing that there is no significant relationship between initial serum AFP levels and prognosis of the patients with HBL (Ortega *et al.*, 1991; von Schweinitz *et al.*, 1994). Moreover, the tumor with low levels of serum AFP often grows rapidly and is often reluctant to chemotherapy (von Schweinitz *et al.*, 1995). The other genetic markers including DNA ploidy, chromosomal aberration, and *p53* mutation are not so powerful clinical indicators. Even the nuclear localization of β-catenin and/or mutation of the *β-catenin* gene appear to lose their impact as a prognostic factor when combined with the grade of histological differentiation because of its close correlation with the latter (Takayasu *et al.*, 2001). Therefore, we may need to find novel markers to predict the patient's outcome in a comprehensive way.

To understand the molecular mechanism of the genesis and progression of HBL, as well as to develop a novel diagnostic and therapeutic system for the tumor, we have randomly cloned 10431 cDNAs expressed in primary HBL tissues and a normal infant's liver by using full-length-enriched oligo-capping cDNA libraries. In the present study, we have identified 86 genes differentially expressed between HBLs and their corresponding normal livers. One of such genes, *PLK1*, showed a significantly high expression in the formers as compared with the latters, and its high expression was significantly associated with poor prognosis of HBLs.

Results

Expression profiles of primary HBLs and a normal liver

To obtain the genes expressed in primary HBLs and normal infant's liver, we constructed oligo-capping cDNA libraries from two primary HBLs with increased AFP secretion (HMFT, HYST), a primary HBL without AFP secretion (HKMT), and a corresponding normal liver (HMFN). After cloning 3000 cDNAs from each of the four cDNA libraries, 2289, 2837, 2537, and 2768 clones from the libraries of HMFT, HYST, HKMT, and HMFN, respectively, were successfully end-sequenced. Homology search against the public databases of those 10431 clones by BLAST program revealed that 847 clones (8.1%) in total contained novel sequences which had not been annotated (Table 1).

To elucidate the gene expression pattern in each cDNA library, we compared expression profile of the known genes that appeared in three different kinds of libraries, a HBL with positive AFP (HMFT), a HBL with negative AFP (HKMT), and an infant's liver (HMFN) (Table 2). BodyMap (Okubo *et al.*, 1992) and a serial analysis of gene expression (SAGE) (Velculescu *et al.*, 2000) are very good methods to quickly provide quantification of the levels of all mRNAs in certain tissues and cell types by high throughput end-sequencing of cDNA clones. In this study, we applied the former method by counting cDNA clones to show each expression profile of HBL tumors or a non-tumorous tissue. Although each library consists of 3000 clones, which may be a rather small number, the frequency of each cDNA appearance provides a hint to understand each tissue's genetic background.

Overall, the most frequently appeared gene was *albumin* as expected, which was extremely low in the tumor with negative AFP. Genes involved in cellular structure and/or maintenance, glucose and lipid metabolisms, and a part of protein synthesis and its transport were frequently found in the normal liver library. On the

Table 1 Summary of the number of genes cloned from the cDNA libraries of hepatoblastomas and a normal infant liver of hepatoblastomas

Oligo-capping cDNA library	*No. of the clones*	*No. of the genes successfully end-sequenced*	*No. of the genes with unknown function*
Hepatoblastomas with positive AFP	6000	5126	323 (6.3%)
Hepatoblastoma with negative AFP	3000	2537	262 (10.3%)
Infant's liver	3000	2768	262 (9.5%)
Total	12000	10431	847 (8.1%)

Table 2 Comparison of the known genes frequently appeared in hepatoblastomas with or without secretion of AFP and a non-tumorous infant's liver

Gene symbol	*Acc. no.*	*Gene name*	*No. of appearance of the genes*		
			HBL with positive AFP	*Normal infant's liver*	*HBL with negative AFP*
Total number of genes			2289	2768	2537
Protein synthesis, metabolism, transport					
ALB	NM_000477	Albumin	558	482	8
AFP	NM_001134	Alpha-feto protein	67	0	0
AGT	NM_000029	Angiotensinogen	43	16	0
EEF1A1	X03558	Eukaryotic translation elongation factor 1 alpha 1	35	20	87
RPL27A	NM_000990	60S ribosomal protein L27a	31	4	52
FTL	M11147	Ferritin	24	11	3
FGA	NM_021871	Fibrinogen, A alpha polypeptide	20	38	2
HP	K01763	Haptoglobin	19	6	1
ORM1	X02544	Orosomucoid-1	12	8	0
RPS27	NM_001030	Ribosomal protein S27	11	4	31
F2	J00307	Coagulation factor 2	11	26	0
TF	NM_001063	Transferrin	8	6	0
PAH	U49897	Phenylalanine hydroxylase	6	6	0
PLG	NM_000301	Plasminogen	5	8	0
SERPINA1	X01683	Serine proteinase inhibitor, clade A, member 1	5	6	0
GC	NM_000583	Group-specific component	4	21	1
RPS29	NM_001032	Ribosomal protein S29	3	1	0
CTSB	NM_147783	Cathepsin B	2	5	3
SERPING1	BC011171	Serine proteinase inhibitor, clade G, menber 1	2	33	0
CRP	X56692	C-reactive protein	1	8	0
ITIH2	NM_002216	Inter-alpha (globulin) inhibitor, H2 polypeptide	0	25	0
Growth factor					
MST1	M74178	Macrophage stimulating 1	8	16	0
Cell signaling					
WIF1	NM_007191	Wnt inhibitory factor 1	0	0	11
DKK1	NM_012242	Dickkopf	0	0	7
Cell structure, adhesion					
VTN	NM_000638	Vitronectin	7	30	0
ACTB	BC013380	Actin	6	17	6
LRG	AF403428	Leucine-rich alpha-2-glycoprotein	6	11	0
VIM	NM_003380	Vimentin	0	3	38
Cell cycle					
RBM4	NM_002896	RNA binding motif protein	2	0	21
RAP1B	NM_015646	RAP1B	0	0	11
Organism defense					
BF	L15702	B-factor, properdin	5	13	0
GPX1	NM_000581	Glutathione peroxidase	4	0	0
C1R	NM_001733	Complement component 1	1	21	1
Glycometabolism					
LDHA	NM_005566	Lactate dehydrogenase	19	28	7
ADH1B	AF153821	Alcohol dehydrogenase	15	29	1
CES1	L07764	Carboxylesterase	9	22	2
ALDH1A1	NM_000689	Aldehyde dehydrogenase	2	13	2
Lipid metabolism					
EPHX1	NM_000120	Epoxide hydrolase 1	7	12	0
APOA2	NM_001643	Apolipoprotein A-II	6	2	0
ADFP	BC005127	Adipose differentiation-related protein	5	14	1
Heat shock protein, metabolic enzyme					
UGT2B4	Y00317	UDP-glucuronosyltransferase	11	32	2
HSPA8	NM_006597	Heat shock 70 kDa protein	1	6	1
Unknown, others					
ATP5A1	NM_004046	ATP synthase	18	11	23
SEPP1	NM_005410	Selenoprotein P	7	10	2